Studies on Polymeric Multilayer: Fabrication and Application to Photonic devices

Redouane Katouf

(Doctoral Program in Applied Physics)

Submitted to the Graduate School of

Pure and Applied Sciences

in partial fulfillment of the requirements

for the Degree of Doctor of Philosophy in Engineering

at the

University of Tsukuba

Studies on Polymeric Multilayer: Fabrication and Application to Photonic Devices

Redouane Katouf

March 2006

Acknowledgment

Many talented people enriched my life and work during my Ph.D. thesis. Any effort to mention all who contributed to this dissertation is bound to remain incomplete. I am, however, grateful for the opportunity to be able to mention at least few of them by name.

My thesis advisor, Prof. Toyohiko Yatagai, has been a constant source of inspiration, guidance and encouragement. He showed me how to be not only efficient but also effective and taught me how to present results in a structured manner. His generous support and confidence gave me the opportunity to present my research results at various conferences in Europe and Japan. Many of his methods have influenced how I work, and without him I would not be where I am today. My thanks go also to his associate professor Masahide Itoh.

I gratefully acknowledge Prof. Shinsuki Umegaki for welcoming me into his group, his numerous insightful discussions, and his encouragement

throughout this thesis. I thank also the members of his group for their friendship; in particular to Toshiyuki Komikado, Izusa Inoue and Naoki Inoue for their discussions, and help during the experiment. It was a great pleasure to work with them for the past two years.

I would like to thank Prof. Kiyoshi Asakawa for serving on my thesis committee. I am greatly honored that he agreed to review this dissertation.

Several people have helped me in various tasks. This include Dr. Majed Abu-Zreig, Mark Tachiki, Dr. Daisuki Barada , and Sadako Yamagata . Thank you for taking time for me.

I would also like to thank the Japanese Ministry of Education which has given

me the chance to come to Japan and provided me with financial support during my studies.

Lastly, I am greatly indebted to my parent, my brother, my two sisters, and all my close friends, without whose understanding and support this dissertation would not exist. I dedicate this dissertation to them with love.

Abstract

One-dimensional photonic crystals, also known as multilayers, are periodic dielectric structures where the period is of the same order of magnitude as the wavelength of light. As a result of interference, Light with certain wavelength at the band gap will be reflected. The polymeric multilayer has many advantages over conventional inorganic ones because it's widely used for fabricating active or novel photonic devices. In addition polymers can be easily processed for various functions by dye doping. In the case of inorganic dielectric materials, the periodic structures were fabricated by vacuum evaporation or sputtering. However, organic polymers can be fabricated by spin coating.

The first goal of this research is the fabrication of multilayer mirrors by spin-coating of high refractive index ratio polymers. A multilayer is formed by stacking a high and low refractive index layers alternatively. In the present experiment, two polymers, poly(vinyl carbazole) and poly(acrylic acid) dissolved in chlorobenzene and diacetone alcohol, respectively, were used as a high and a low refractive-index layers. Optical thickness of layers at $\lambda/4$ was controlled by adjusting the concentration of solutions and by changing the rotation speed of spin-coating. Experimental results revealed an increasing reflectivity with an increase in the number of layers through a repetitive process of spin-coating and solvent drying. Reflectivity more than 95% was observed at designed wavelength of 1064 nm by stacking only 35 layers.

The second goal is the fabrication of an electro-optic and an all-optical devices by doping a polymeric multilayer with a second and third order nonlinear dye. The electro-optic device, operating at 1064nm was manufactured by simple spin coating and baking of alternatively PVK as high refractive index and DR1 doped PAA as low

refractive index at quarter wavelength optical thickness. Transmission change of 30% was achieved using this device as a switch by applying a voltage of 100V/μm..

The all-optical device was fabricated, based on the properties of Kerr-nonlinear polymeric multilayer. The device was fabricated by doping 3^{rd} order nonlinear Styryl 9M in both layers, PVK and PAA, constructing the multilayer, and a poly-orange tom-1 was used as a defect layer. The defect peak in the band gap could be shifted by applying a control beam. Thus, it performs an all-optical switching function at which the probe beam can be dynamically reflected depending on the control beam. The device acted as an optical switch, showing the transmission change of 44% by use of 3kW/cm^2 pump beam.

Contents

List of Figures

Chapter 1

General Introduction

Over the last two decades, advances in electronics have revolutionized the speed with which we perform computing and communications of all kinds Three key technologies combined to create a platform that enabled the electronic revolution: semiconductor materials, automated micro-fabrication of integrated electronic circuits, and integrated electronic circuit design. As a result, the mass manufacturing of low-cost integrated circuits has become possible. The trend for even higher density of integration and faster processors pushes the miniaturization to the extreme for electronic devices. The high resistance and therefore long delay time associated with the small feature size, and the synchronization problem arising from high speed transmission of data becomes more and more serious for electronic devices, so now we are outgrowing the performance of electronics in many applications. Signal propagation and switching speeds in the electronic domain are inherently limited. One area where these limitations are seen clearly is in telecommunications, where bandwidth expansion is desperately needed. To overcome these barriers, we must enter a new computing and communications revolution-this time based on photonics.

At this turn of the century, just as semiconductors have revolutionized the electronics technology, in a way never envisaged at the time when the transistor was invented[1],[2]. Photonic crystals, being the optical analogue of electronic semiconductor crystals, might lead to a major breakthrough in optoelectronics and integrated optics. There is a possibility that photonic devices may replace electronic devices. Due to the high frequency nature of the light, the available bandwidth of photonic devices is higher than conventional electronic devices. In photonic devices the loss of power can be reduced to minimum by proper choice of the medium.

Photonics play some crucial and complementing roles to electronics in many application domains. Examples of successful use of photonics can be found in broadband communications, high-capacity information storage, and large screen and portable information display. As demands for information bandwidth increase, information photonics is becoming more and more important in every aspect of today's technology-driven society. The success of a new technology, however, largely depends on the progress achieved in finding and fabricating new high- performance and cost-effective materials. Recently, as the knowledge base of polymeric materials widened, new functions for polymers have been actively investigated. New and improved polymeric materials were found to show promises in generating, processing, transmitting, detecting, and storing light signals.

Nonlinear optical (NLO) materials, especially organic and polymeric ones, have continued to be at the forefront of research activities since the mid-1980s. Moderate NLO susceptibility, fast response time, low dielectric constants, small dispersion in the index of refraction from dc to optical frequencies, virtually endless possibilities of structural modification, and ease in processibility are some of the properties of conjugated organic systems uniquely suited for their applications in photonic devices, such

as the frequency converters, high-speed electro-optic (E-O) modulators and switches. In particular, a low half-wave voltage (Vp) of 0.8 V has been achieved recently in a polymer waveguide modulator using highly nonlinear organic chromophores and push-pull poling and driving techniques [3]. This discovery, together with a recent demonstration of exceptional bandwidths (as high as 150 GHz) [4] and ease of integration with very large scale integration (VLSI) semiconductor circuitry and ultra-low-loss passive optical circuitry, have provided a solid foundation for using polymeric materials in next-generation telecommunications and information processing.

It is well-known that the second-order NLO properties originate from non-centrosymmetric alignment of NLO chromophores, either doped as a guest or covalently bonded as side-chains in poled polymers. To obtain device-quality materials, three stringent issues must be addressed:

1. Design and synthesis of high mb (m: the chromophore dipole moment, b: the molecular first hyperpolarizability) chromophores and realization of large macroscopic E-O activity in the chromophore-incorporated polymers;

2. Maintenance of long-term temporal stability in the E-O response of the poled materials in addition to their high intrinsic stability toward the environment such as heat, light, oxygen, moisture and chemical;

3. Minimization of optical loss from design and processing of materials to fabrication and integration of devices.

1.1 Technologies of the Future

1.1.1 Photonic devices

Any forecast about the promise of a communications technology must include an appreciation of its place within the larger communications ecosystem in which it will exist. This ecosystem comprises key elements such as transmission, distribution, switching, processing, storage, and display. Development of a viable communications infrastructure requires that those elements scale together. Photonic technology holds great promise for realizing this coordinated scaling within future high-speed communications from the chip level through board interconnects, to enterprise and long haul. The key is to identify commonalities that drive scale and build the technical infrastructure necessary to enable optical technology to replace electrical devices. As the end-to-end infrastructure becomes increasingly optical, network latency will decrease to the point that communications become perceptually instantaneous to users. Optical networks will enable sophisticated applications such as transmission of "presence" in teleconferencing, computer-assisted surveillance, instant access to multimedia, real-time weather telemetry in navigation, and cost-effective Lidar for autos. The implications are enormous.

Today, digital networks operate at greater capacity and speed; but despite the fact that optical fiber has been used since the 1980s, current networks are still limited by the electrical interconnects at their termini. The opportunity to advance the speed of communications lies in replacing these slower components with photonic equivalents. The realization of optical transmission networks will allow any connected individual to access vast computational resources. Unbounded applications, not dependent upon local storage or processing, will be limited only by the imaginations of those

who create them. Many of the current economic and distribution barriers between intellectual property owners and end-users will evaporate. Ubiquitous computing and communications will revolutionize medicine, education, and social interaction. The effect of such technology on transportation, commerce, education, entertainment, social interaction, and government will be dramatic. For instance, one only needs to look at the world ten years ago to understand the social impact of the cell phone. The shift to a real-time wideband network promises the same dramatic social effect. Many enabling components already exist in laboratories. The demand created by new long-haul networks will allow them to be applied on a commercial scale. With the advent of this new communications infrastructure, 21st century society will be witness to a renaissance of applications spawned from the ability to extend computer-moderated information directly to the end user in real-time. Third generation applications will fuel the information vehicles. Photonics will speed the underlying highway.

The current standard of 'fiber pigtail' packages is inconsistent with planar integration. Receptacle connectors will require self-cleaning to be effective. An optical chip carrier without permanent fiber attach is absolutely necessary. A common design hierarchy for board, backplane, intrabox, interbox, LAN, FTTH, MAN, and WAN applications will be developed (Fig 1.1). The overarching expectation is that such technology will be then driven by technology obsolescence through performance scaling, with products lifetime significantly shorter than the network cycle. Optical communication technologies provide the ultimate performance for speed, reliability, and security. Microphotonic integration provides instant access to the greatest virtual repository of information ever.

The Network Photonics press release is quite important because it focused on the heart of optical network switches. Network Photonics is using the O-E-O (Optical-

	1990	2000	2010	2020	2030
PHOTONICS					
Driver	Fiber, lasers, detectors	MUX, EDFA	Metro-fiber, PLC Transceiver	µPh ICs FTTH	Pervasive, µPh ICs
Transmission Application	ETDM WAN	DWDM WAN	Security Access SAN/LAN	1 Gb/s Access 10 Tb/s WAN	Optical switching systems
Trend	Fiber	Fiber pigtail	Boards, Servers	Optical MCM	Optical nodes
ELECTRONICS					
Driver	IC: Al/SiO_2 GaAs	IC: Cu/SiO_2 InP	Optical bus	On-chip optical interconnects	Optical switch
Processing Application	S/DRAM, ASIC, µProc MIMIC	DSP µProc TIA	Parallel processing	EP signal conditioning	EP signal processing
Trend	Yield Yield	Shrink Yield	Optical interconnection	EP design	Photonic logic

Figure 1.1: Roadmap for electronic-photonic convergence; dates represent decade for commercial deployment. (EDTM: electronic time domain multilexing, DWDM: dense wavelength division multiplexing, SAN: storage area network, WAN: wide area network, MCM: multi-chip module, FTTP: fiber to the home, EP: electronic photonic) [Source: MIT Microphotonics, "communications technology roadmap 2005"].

Electrical-Optical) arrangement in most optical systems which change optical to electrical and back to optical in order to monitor, control and switch the optical data stream. Going all optical has the potential of increasing the bandwidth significantly for the entire network. This technology will certainly be the question of Optical Interconnect growth in backplane technology for large servers. Going O-O-O still requires a transition to electrical, and at that point signal integrity requirements will be even higher.

Wavelength based architecture requires fast wavelength converters. All optical signal processing evolution will bridge the gap toward transparent optical networking such as header recognition, logic gate etc. New applications may rise up from research

using photonic band-gap devices such as all-optical devices and electro-optic devices that will share various parts of the network.

Materials used for photonic devices are silicon, III-V(InP, GaAs), and organic. III-V material systems possess properties that achieve superior optical device performance, which cannot be achieved currently by silicon-based materials, however, current processing, cost, and design paradigms for the III-V material do not support the yield and functionality necessary for integration in future devices, where the low cost and high-volume manufacturing will become the dominant issue for the materials. The key challenges for a cost-effective, planar technology are large area substrates and component integration capability. In the other hand, Organic materials can be processed with reduced temperature excursions. This property allows rapid manufacturing and ease of integration.

1.1.2 Organic materials

In the case of materials for future photonic devices, studies of both organic and inorganic materials are pursued. Organic materials might provide systems developed with unique possibilities and higher flexibility in comparison with inorganic materials because of the relatively easy way to process organic polymeric materials into practical devices [5],[6],[7],[8].

Organic materials can accomplish the full array of optical functions and can be processed at temperatures that are compatible with CMOS integrated circuits. Passive dynamic organic photonic components with cutting edge performance and proven reliability are commercially available today, whereas active organic photonics and organic electronics are less mature and are not yet capable of high performance. Over

the next decade, organic materials will continue to be an indispensable ingredient in hybrid integrated photonic circuits and will play a key role in meeting market needs for low-cost, large-volume photonic components. Electronic-photonic integration is the major trend that is driven by complexity, performance, and cost. The low thermal budget for organic material devices fabrication makes them ideal components for advanced electronic-photonic partitioning.

Material System	Propagation Loss (dB/cm)	Pigtail Loss (dB/chip)	Refractive Index (n)	Index Contrast Range in Waveguide (Δn)	Birefringence ($n_{TE} - n_{TM}$)	T/O Coef. dn/dT (K^{-1})	Maximum Modulation Frequency
Silica [SiO_2]	0.1	0.5	1.5	0 ~ 4% (Channel)	$10^{-4} \sim 10^{-2}$	10^{-5}	1 kHz (T/O)
Silicon [Si]	0.1	1.0	3.5	70% [range = 0] (Silicon on Insulator Rib)	$10^{-4} \sim 10^{-2}$	1.8×10^{-4}	1 kHz (T/O)
Silicon Oxynitride [SiO_xN_y]	0.1	1.0	SiO_2:1.5 Si_3N_4:2.0	0 ~ 30% [30%: Si_3N_4 core]	$5\times10^{-6} \sim 10^{-3}$	10^{-5}	1 kHz (T/O)
Polymers	0.1	0.2	1.3 ~ 1.7	0 ~ 35% (Channel)	$10^{-6} \sim 10^{-2}$	$-1 \sim -4\times10^{-4}$	>100 GHz (E/O) 1 kHz (T/O)
Lithium Niobate [$LiNbO_3$]	0.5	2.0	2.2	0 ~ 0.5% (Channel)	$10^{-2} \sim 10^{-1}$	10^{-5}	40 GHz (E/O)
Indium Phosphide [InP]	3	10	3.1	0 ~ 3% (Channel)	10^{-3}	0.8×10^{-4}	40 GHz (E/O)
Gallium Arsenide [GaAs]	0.5	2.0	3.4	0 ~ 14% [14%: AlAs clad]	10^{-3}	2.5×10^{-4}	20 GHz (E/O)
Garnets [e.g. YIG]	0.5	2.0	2.2	0 ~ 12% [12%: GGG clad]	$10^{-5} \sim 10^{-4}$	10^{-5}	N/A

Figure 1.2: Properties of key integrated optical material systems.[9]

Organic polymers are a compelling choice as the base material for a hybrid integration platform because, when synthesized and processed properly (Fig. 1.2), they offer high performance (the transparency of state-of-the-art polymers is on par with that of silica [$\leq$ 0.1 dB/cm at all communication windows] and the birefringence is smaller than that of silica by two orders of magnitude), wide controllability of the refractive index contrast (the maximum Δn is an order of magnitude larger than that achievable in silica), tunability (the thermo-optic coefficient is more than an order of magnitude larger than that of silica), environmental stability, ease of hybridization, high yields, and low cost. In order for polymers to be usable in the commercial production of photonic components, new devices have to be developed using 2^{nd} and 3^{rd}

order nonlinear chromophores doped polymers.

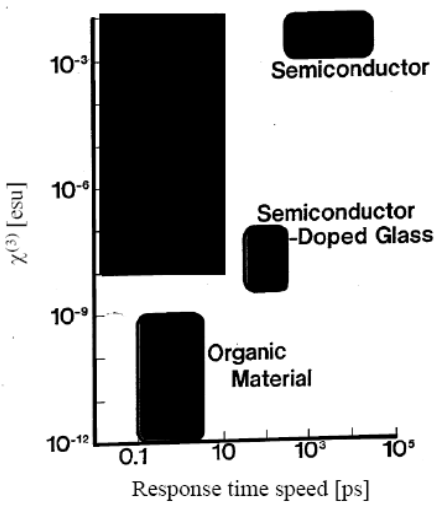

Figure 1.3: Imporatnt parameters in 3rd order nonlinear optical materials

In nonlinear polymer, the effects are electronic, which assures, in combination with a low dielectric constant, the very high-speed operation required for future communication systems, however, they still suffer from a low 3^{rd} order nonlinear susceptibility (Fig. 1.3) compared with semiconductor. But, they have exceptionally high 2^{nd} order nonlinear activity, EO coefficients up to 34pm/V have been reported in poled polymeric films and devices, which compares favorably to competing technologies such as lithium niobate ($LiNbO_3$) with a highest EO coefficient (r_{51}) of 32pm/V. As a result, polymeric materials promise to make optoelectronic technologies more practical and widespread. they could make major impacts on communication [10] if combined with photonic crystal technology.

1.2 Aims of this work:

Demands for ultra-high-speed and ultra-high-capacity optical communications and optical data processing systems are increasing dramatically. There are high interests in electro-optic and all-optical ultrafast photonic devices that are needed for future optical communications.

Fabricating three-dimensional photonic crystals at present is complicated, since the control of the dielectric constant with spatial precision higher than the wavelength of light is very difficult. In many applications, however, the control of laser beams is required where laser beams are close to plane waves. In this case, one-dimensional photonic crystals (1-D PCs) or dielectric multilayers are sufficient. Furthermore, the dielectric multilayer is the best solution for the enhancement of optical nonlinearities, because the incident light field can be fully coupled to the localized defect mode. Fabricating multilayers by the use of doped polymers can produce various active devices for future applications in optical communications.

The first aim of this thesis, is development and improvement of spin coating method to fabricate high reflection multilayered mirror by stacking high refractive index ratio polymers as high and low refractive index layers, alternatively. The second objective is to dope the polymeric multilayer with 2^{nd} and 3^{rd} order nonlinear chromophores to fabricate active devices like electro-optic devices and all-optical devices. These devices have great widespread application in optical communications and optical signal processing applications, due to their light weight, compactness and low production cost.

This thesis is divided into two parts, the first part describes the fabrication process of polymeric multilayer by spin coating and process improvement steps. The second

part describes the fabrication of electro-optic device and all-optical device obtained by 2nd and 3rd order dyes doped polymeric multilayer.

Chapter 2

Photonic Crystals

2.1 Introduction

Photonic crystals are periodic structures made of dielectric materials. Regions with different dielectric constants alternate periodically and the period is of the order of the wavelength of light. Photonic crystal possesses a periodic index of refraction along one, two or three axes (Fig 2.1). Then, as light propagates inside the periodic material, it reflects at each interface of the different dielectric materials. As a result of interference, total reflection occurs at specific wavelength-period combinations. Light with this specific wavelength cannot propagate or exist inside the photonic crystal. These forbidden wavelengths or frequencies form a band gap for light, which is the basis of operation of photonic crystals. This phenomenon is also present in the nature: The wings of certain butterflies and moths are covered with periodic microscopic structures, which act as photonic crystals [11]. The wings reflect light that has a wavelength in the band gap of the photonic crystal. This effect is seen as the color of the wings. Also, one-dimensionally periodic structures have been widely

used for a long time in various optical components. Well known applications are for example Bragg mirrors and optical filters.

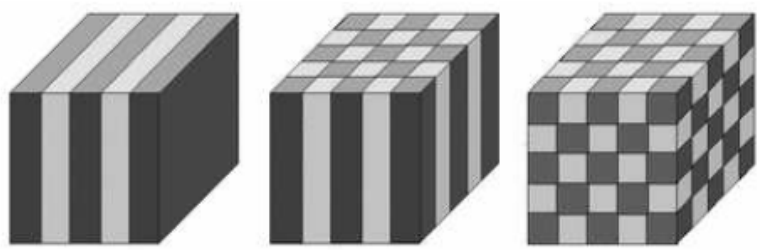

Figure 2.1: Simple examples of one-, two-, and three-dimensional photonic crystals. The different colors represent materials with different dielectric constants.

The concept of photonic crystals was starting to emerge at the end of the 80's, when it was realized that the effect of three-dimensionally periodic media to light can be thought of being somewhat similar to the effect of semiconductors to electrons [12][13]. This opened new prospects in photonics. It was realized that the electromagnetic band gap for light would prohibit spontaneous emission [12] or light could be localized when disorder is present in a periodic medium [13]. The experimental search for a photonic band gap structure begun [14]. Meanwhile, the theorists calculated the band structure for light, similar to the electronic band structure in semiconductors, and it was shown that a three-dimensional photonic band gap would exist in a diamond lattice of dielectric spheres [15]. The first three-dimensionally periodic structure exhibiting a photonic band gap in the optical wavelength range was fabricated in the beginning of the 90's [16]. It was called Yablonovite, named after E. Yablonovitch, the inventor of the structure. It was fabricated by drilling three sets of holes in specified angles into a solid slab of semiconductor and had a band gap in the microwave region. Implanting defects into Yablonovite [17] and the possibility of a single-mode light-emitting diode (LED) using a photonic crystal cavity were

envisioned [18].

2.2 Properties and applications:

Since the realization of a three-dimensionally periodic structure with micrometer size features was very difficult, there were experiments [19][20] and theory [21][22] done with two-dimensionally periodic structures exhibiting band gaps. A true photonic crystal is periodic in all three directions and thus can have such a band gap that light is not allowed to propagate in any direction. However, structures that are periodic in only one or two dimensions are also called one- and two-dimensional photonic crystals, respectively. Although they are not photonic crystals in the strict sense, they posses similar properties, only in the direction of the periodicity. Line defects in two-dimensional photonic crystals were predicted to act as waveguides, and point defects as microcavities [23]. In these new photonic crystal waveguides light would follow a sharp 90 degree bend with almost 100% transmission over a broad frequency range [24]. It was not until the end of the 90's when a structure with a photonic band gap in the infrared frequencies was first realized with a face-centered-cubic lattice of metallic squares [25]. It was not very applicable at optical wavelengths, however, due to strong attenuation. Band gap in the infrared frequencies with a dielectric structure was first realized with the woodpile structure that consists of tiny rods of silicon piled up in a layer by layer manner [26]. The same geometry was also used to construct the first photonic crystal for the wavelengths used in the telecommunications, 1.3 and 1.5 μm [27]. In order to incorporate active photonic devices, the woodpile structure was also fabricated from GaAs and InP instead of silicon [28].

Nowadays, three- and two-dimensional photonic crystals can be fabricated with

established fabrication methods and various components have been realized [29], [30], [31], [32]. Two-dimensional photonic crystals and photonic crystal slabs, which have a finite thickness in the vertical direction, have been used to fabricate for example waveguides [33][34], microcavities [35], [36], [37], add-drop devices [38], and lasers [39], [40], [41]. Three-dimensional photonic crystals have been used for microcavities, light-emitting diodes (LEDs) and lasers [42]. Nonlinear photonic crystals have been demonstrated to exhibit all-optical switching behavior and optical bistability [43].

Photonic Crystals fully employ the coherent nature of the light, and open a new area of promise for the development of all optical integrated circuits.

Many interesting properties have been predicted for photonic crystals. they allow to control spontaneous emission, a parasitic process in many optoelectronic devices, and control and manipulate the flow of light. Both characteristics imply that photonic crystal would be an ideal material for making optical circuits. One could build extremely efficient micron-scale optical waveguides, cavities, and mirrors, that could be integrated in optical "chips".

2.3 Fabrication methods:

The most popular 3D photonic crystal has been the woodpile structure [44], [45], [46]. Some 3D photonic crystals are fabricated by repetitive deposition and etching of multiple dielectric films of silicon using well developed and supported Si integrated circuit fabrication processes. Structures consisting of III-V semiconductors have been fabricated by stacking stripe-patterned wafers with a precise alignment technique and wafer-fusing them [47], [48]. Since the woodpile structures are fabricated with lithographic procedures, their thickness in the growth direction is only a couple of unit

cells. Larger woodpile structures have been produced by preparing unit plates using a single sequence of an integrated circuit process and then accurately aligning the lattices by micromanipulation [49]. Considerably larger three-dimensionally periodic structures can be fabricated by spontaneous crystallization of colloids, i.e., hard particles in suspension. The polymer or silica microspheres naturally self-assemble from colloidal suspension into a solid, three-dimensionally periodic structure, which can then act as a template for construction of the photonic crystal. Photonic crystals exhibiting complete band gaps near 1.5 μm [50] and 1.3 μm [51] were fabricated by synthesis of silicon inverse-opal structure. Lattice of mono-disperse silica spheres was used as a template for silicon infiltration. Silicon was grown inside the voids of the opal template by means of chemical vapor deposition and the silica template was subsequently removed. The drawback of the inverse-opal structures is that the band gap is small due to the face-centered-cubic and hexagonal-close-packed geometries. Also the purity of the structures has been poor.

Another method to fabricate large-scale 3D photonic crystal structures with submicrometer periodicity is the 3D holographic lithography [52], [53]. In holographic lithography, a film of photoresist is illuminated by the interference pattern of four non-coplanar laser beams and the unexposed areas are subsequently dissolved. This results in polymeric structures, which are used as templates to create complementary dielectric structures with high refractive-index contrast. However, the inclusion of defects in the periodic structures constructed by holographic or self-assembly methods is difficult.

Large photonic crystals of square spiral posts in a tetragonal lattice have also been proposed to be conceivable by large scale microfabrication using glancing angle deposition techniques [54]. The technique combines oblique vapor deposition and

precisely controlled motion of a two-dimensionally patterned substrate.

There are also other layer-by-layer structures exhibiting 3D photonic band gaps that can be fabricated by lithographic methods. One consists of an alternating stack of 2D photonic crystal structures: dielectric rods in air and air holes in dielectric where designed point defects can be flexibly introduced [55], [56]. Another proposed geometry consists of alternating layers of rods and veins [57].

The first 2D photonic crystals were fabricated by micro-assembly, which was feasible due to the large enough size of the dielectric cylinders [58] and the aluminaceramic rods. These photonic crystals operated in the centi- and millimeter wavelength range. However, more sophisticated fabrication methods are needed when the structures are scaled down. Macroporous silicon was demonstrated to have a band gap centered at 5 μm [59]. It was fabricated by electrochemical etching in hydrofluoric acid and resulted in uniform pores with a diameter in the micrometer range and a depth of several hundreds of micrometers. Two-dimensional band gap in the visible wavelength range was shown in nanochannel glasses which are a regular array of air cylinders fabricated by a fiber draw process [60]. The most popular way to fabricate 2D photonic crystals is, however, electron beam lithography and etching of semiconductor materials. A 2D photonic crystal for 1.47-1.6μm has been fabricated by electron beam lithography and dry etching on a GaInAsP thin film [61]. A 2D photonic crystal slab has been fabricated by first growing a semiconductor (InGaAsP) layer by metal-organic vapor phase epitaxy. Then a resist mask, with the photonic crystal pattern, was coated on the semiconductor layer by electron beam lithography and the resist pattern was transferred to the semiconductor layer by reactive ion etching [62].

Many research are focused in the study of one-, two- and three-dimensional photonic crystal, however of special interest in this thesis is one-dimensional photonic

crystals known also as distributed Bragg reflector and multilayer mirror.

Part I

Multilayer Structures

Chapter 3

Introduction

Over the past decade or so, there has been intense interest in the transmittance and reflectance properties of multilayered structures of various solid materials. In that time, substantial theoretical and experimental research has been done to analyze the transmission properties of multilayered, periodic (so called "Photonic Band Gap"). These structures take advantages of combinations of materials with differing indices of refraction combined in multilayer periodic fashion to obtain an optical structure with interesting transmission properties. Periodic structure typically would one-dimensional stack of repeating "unit cells" consisting of layers of two materials differing significantly in index of refraction. If one of the materials in the photonic bandgap structure is an optically "active" nonlinear material (that is, it has a nonlinear electric susceptibility $\chi^{(2)}$or $\chi^{(3)}$), the result can be a very inexpensive electro-optical and all optical devices with greatly enhanced conversion efficiency in a very compact space.

Well-known optics theory indicates that a ray of light incident on the boundary of two materials of differing index of refraction will be partially reflected and partially

transmitted. However, only in relatively recent years have manufacturing techniques been developed to allow the production of devices which can take full advantage of these effects. Thin layers of an appropriate material can be applied in conjuction with optical surfaces to eliminate unwanted reflection such as in showcase glasses or high-quality camera lenses. On the other hand, a multilayered structure can be made to be anti-reflective at a desired wavelength in applications such as nonabsorbent beam splitters and dichroic mirrors, transmitting the desired wavelength and reflecting others. Multilayer narrow band-pass filters can be made to transmit light over a specific spectral range, and find a multitude of practical applications. In optical communications, fiber Bragg gratings are used as filters, reflecting some wavelengths of light while letting others through. In laser systems, multilayer structures can be employed as efficient reflectors. In polarizers they can be used to polarize natural light. In bistable structures that employ nonlinear materials, a periodic multilayer superlattice can be constructed producing applications in optical logical functions. In all, multilayer structures have found numerous applications in many aspects of photonics.

Of interest in this work is one dimensional structure made up of alternating layers of two materials one of a fairly higher index of refraction than the other. The complete structure is made up of N "unit cells" (the two layer repeating unit) preceded by an incident medium (usually air) and transmitting medium, or substrate (usually a glass). This kind of structure is shown in Figure 3.1.

When light is incident on the type of structure described above, the transmission spectrum exhibits frequency regions where energy is freely transmitted or prohibited. A simplified plot of transmittance versus wavelength for such structure is shown in Figure 3.2. Because there are wavelength ranges where the incident wave is not

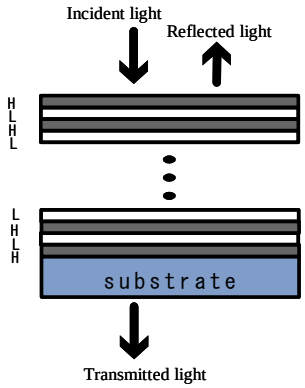

Figure 3.1: Shematic of Multilayer structure

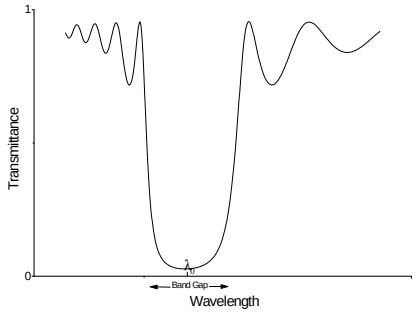

Figure 3.2: Simple Transmittance Spectrum for a one dimensional PBG Material

transmitted, these structures have become known as "Photonic Band Gap" or "PBG" materials. the reflectance/transmittance properties of the structure can be "tuned" by designing the layers at thicknesses associated with the wavelength of light λ_0 desired to be reflected or transmitted. The band gap is centered at the reference wavelength and its width is a sensitive function of the number of periods, the values of n_1 and n_2 and their relative difference $\delta n = |n_1 - n_2|$ sometimes called the index modulation depth.

Factors responsible for improving their reflectivity were clearly identified based on mathematical derivations and proofs [63]. One of these factors dictates that the design

of each layer of the structure must have an optical thickness that is a quarter of the design wavelength, $\lambda/4$. The design wavelength refers to the wavelength at which a resonance is sought. A structure with $\lambda/4$ geometry results in the maximum possible reflection by each layer. Another important factor is the index contrast between the two constituent materials that make up the structure. The larger it is, the higher the reflectivity of the structure. This factor, for example, is important in the design of periodic multilayer. In addition, the more periods there are in a periodic structure, the higher the total reflectivity.

With appropriate design considerations, practical use can be made of the "band gap" properties of these structures. For example, a nonlinear device can be designed that at high incident intensities, will limit the optical frequencies usually transmitted at lower power (an optical limiter), A novel optical switch can be designed by combining the appropriate PBG material with a control beam or driving voltage and other nonlinear optical inclusions to turn a device on or off at frequency at the defect peak or at the edge of the band gap.

Periodic multilayers are generally fabricated using inorganic dielectric materials like T_iO_2 and S_iO_2 by vacuum deposition, because of their large refractive index ratio ($n_{T_iO_2}$=2.5 and $n_{S_iO_2}$=1.45), Although the fabrication apparatus cost very high and it needs careful control of partial pressure and temperature of reactive gas.

Chapter 4

Theory

4.1 Wave propagation

The usual way to understand the properties of the wave propagation in periodic multilayer is to analyze solution of Maxwell's equations in the periodic system. Using Maxwell's equation we can set up a wave equation or, in the stationary case, a Helmholtz equation:

$$(\Delta + (\omega/c)^2\varepsilon(x))E_k(x) = 0,\ \varepsilon(x) = \varepsilon_0 + \varepsilon_1(x) \tag{4.1}$$

where $\varepsilon_1(x)$ is a periodic function: $\varepsilon_1(x) = \varepsilon(x + R)$. Because of the periodicity of the medium we can expand the function $\varepsilon_1(x)$ in a Fourier series on the reciprocal lattice vector:

$$\varepsilon_1(x) = \sum_G U_G e^{iGx}, \tag{4.2}$$

here U_G is the amplitude of the oscillation of the dielectric constant, and G is the

reciprocal lattice vector. Also the electric field can be expand in a Fourier series on the vectors G:

$$E_k(x) = \sum_\alpha \sum_G E^\alpha_{k-G} \exp[i(k-G)x], \tag{4.3}$$

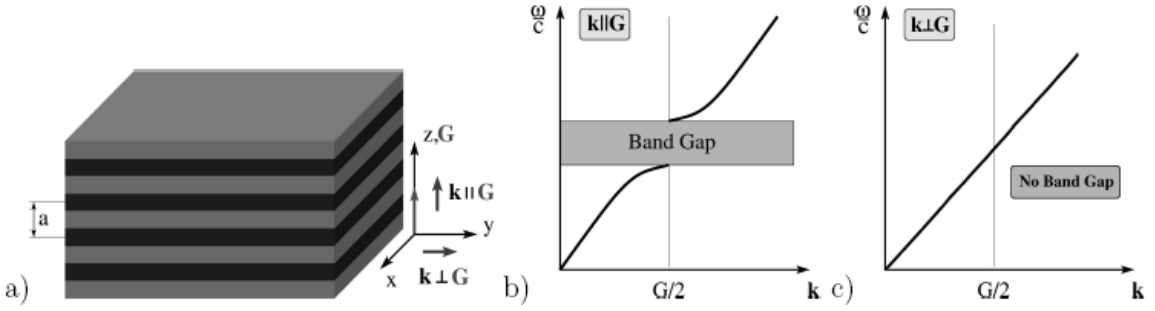

Figure 4.1: Periodic multilayer - DBR (a). Illustration of photonic band gap phenomena (b,c).

where α is the index of photon polarization. Any polarization can be expanded on two components: $\alpha = (x, y)$ for linear polarization, or $(+, -)$ for circular photon polarization.

Due to space inhomogenety the harmonics E^α_{k-G} are coupled. Through introducing (4.2, 4.3) into (4.1) we obtain approximate amplitude equations for the harmonics:

$$\sum_\alpha E^\alpha_k [k^2 - (\omega/c)^2 \varepsilon_0] = \sum_\alpha (\omega/c)^2 \varepsilon_1 (U_G E^\alpha_{k-G} + U_{-G} E^\alpha_{k+G}), \tag{4.4}$$

$$\sum_\alpha E^\alpha_{k-G} [(k-G)^2 - (\omega/c)^2 \varepsilon_0] = \sum_\alpha (\omega/c)^2 \varepsilon_1 (U_{-G} E^\alpha_k + U_G E^\alpha_{k-2G}), \tag{4.5}$$

which are valid when $\varepsilon_1(x)$ is rather small.

Let us discuss the periodic multilayer (Fig 4.1(a)). For the case of normal incidence

($k \parallel G$), all polarizations are decoupled and Eqs.4.5 become scalar. Near the band edge ($k \approx G/2$) only the scattering from the 1st Bragg plane is important:

$$E_k^\alpha[k^2 - (\omega/c)^2\varepsilon_0] = (\omega/c)^2\varepsilon_1 U_G E_{k-G}^\alpha, \tag{4.6}$$

$$E_{k-G}^\alpha[(k-G)^2 - (\omega/c)^2\varepsilon_0] = (\omega/c)^2\varepsilon_1 U_{-G} E_k^\alpha, \tag{4.7}$$

These equations result in the following dispersion relation:

$$[k^2 - (\omega/c)^2\varepsilon_0][(k-G)^2 - (\omega/c)^2\varepsilon_0] - (\omega/c)^4\varepsilon_1^2 U_G U_{-G} = 0 \tag{4.8}$$

When $k = G/2$ and $U_G = U_{-G}$ we get

$$\omega_\pm/c = k/\sqrt{\varepsilon_0 \pm \varepsilon_1 U_G} \tag{4.9}$$

Thus the forbidden band gap appears at the edge of the Brillouin zone (Fig. 4.1(b)) $\Delta\omega = \omega_- - \omega_+ \approx \omega\,|\varepsilon_1 U_G|\,/\varepsilon_0$. The picture changes drastically when the light propagates parallel to the layers. In this case a photonic band gap does not appear (Fig.4.1(c)).

The above example shows that properties of a periodic multilayer depends strongly on the direction of the incident light. In the next section we will review the reflection of multilayers.

4.2 Reflection

The boundary condition, using the matrix formalism for the transverse electric (TE) and the transverse magnetic (TM) waves incident on the interface of two optical mediums of refractive indices n_1 and n_2, are as follows [64]:

(i) TE wave:

$$E_1 + E_1^{'} = \widetilde{E}_2 + \widetilde{E}_2^{'} \tag{4.10}$$

$$(H_1 + H_1^{'})cos\theta_1 = (\widetilde{H}_2 + \widetilde{H}_2^{'})\cos\theta_2. \tag{4.11}$$

Using $H = \sqrt{\frac{\varepsilon}{\mu}}E, \mu = 1$, and $n = \sqrt{\varepsilon}$, Eq.(4.11) can be rewritten as

$$n_1 \cos\theta_1 (E_1 - E_1^{'}) = n_2 \cos\theta_2 \left(\widetilde{E}_2 - \widetilde{E}_2^{'}\right) \tag{4.12}$$

Therefore Eqs (4.10) and (4.12) can be combined to yield

$$\begin{bmatrix} 1 & 1 \\ n_1\cos\theta_1 & -n_1\cos\theta_1 \end{bmatrix} \begin{bmatrix} E_1 \\ E_1^{'} \end{bmatrix} = \begin{bmatrix} 1 & 1 \\ n_2\cos\theta_2 & -n_2\cos\theta_2 \end{bmatrix} \begin{bmatrix} \widetilde{E}_2 \\ \widetilde{E}_2^{'} \end{bmatrix} \tag{4.13}$$

(ii) TM wave:

$$(E_1 + E_1^{'})\cos\theta_1 = (\widetilde{E}_2 + \widetilde{E}_2^{'})\cos\theta_2, \tag{4.14}$$

$$H_1 + H_1^{'} = \widetilde{H}_2 + \widetilde{H}_2^{'} \tag{4.15}$$

Using $H = \sqrt{\frac{\varepsilon}{\mu}}E, \mu = 1$, and $n = \sqrt{\varepsilon}$, Eq. (4.15) becomes

$$n_1(E_1 - E_1^{'}) = n_2\left(\widetilde{E}_2 - \widetilde{E}_2^{'}\right); \tag{4.16}$$

Equation (4.14) and (4.16) are combined to give

$$\begin{bmatrix} \cos\theta_1 & \cos\theta 1 \\ n_1 & -n_1 \end{bmatrix} \begin{bmatrix} E_1 \\ E_1^{'} \end{bmatrix} = \begin{bmatrix} \cos\theta_2 & \cos\theta_2 \\ n_2 & -n_2 \end{bmatrix} \begin{bmatrix} \widetilde{E}_2 \\ \widetilde{E}_2^{'} \end{bmatrix} \tag{4.17}$$

For a TE wave, the dynamical matrix is defined as

$$D_i = \begin{bmatrix} 1 & 1 \\ n_i\cos\theta_i & -n_i\cos\theta_i \end{bmatrix} \tag{4.18}$$

For a TM wave, the dynamical matrix is given by

$$D_i = \begin{bmatrix} \cos\theta_i & \cos\theta_i \\ n_i & -n_i \end{bmatrix}. \tag{4.19}$$

where $E_i\,(H_i)$ and $E_i^{'}\left(H_i^{'}\right)$ represent the forward and backward electric (magnetic) fields of the ith medium at the ith interface. θ_i is the incident angle of the ith medium; θ_{i+1} is the refractive angle in the $(i+1)$th medium. Similarly, $\widetilde{E}_{i+1}\left(\widetilde{H}_{i+1}\right)$ *and* $\widetilde{E}_{i+1}^{'}\left(\widetilde{H}_{i+1}^{'}\right)$ represent the forward and backward electric (magnetic) fields at the $(i+1)$th medium at the ith interface. The relation between $E_i\left(E_i^{'}\right)$ and $\widetilde{E}_{i+1}^{'}\left(\widetilde{E}_{i+1}\right)$ can be rewritten as

$$D_1\begin{bmatrix} E_1 \\ E_1^{'} \end{bmatrix} = D_1\begin{bmatrix} \widetilde{E}_2 \\ \widetilde{E}_2^{'} \end{bmatrix} \Rightarrow \begin{bmatrix} E_1 \\ E_1^{'} \end{bmatrix} = D_1^{-1}D_2\begin{bmatrix} \widetilde{E}_2 \\ \widetilde{E}_2^{'} \end{bmatrix} \tag{4.20}$$

The electromagnetic field gains a phase factor of $\varphi_i = 2\pi n_i d_i\cos\theta_i/\lambda$ in the ith

medium if it propagates through a distance of d_i. Therefore, the relation between $E_i\left(E_i^{'}\right)$ and $\widetilde{E}_i\left(\widetilde{E}_i^{'}\right)$ is given by the following equation:

$$\begin{bmatrix} \widetilde{E}_i \\ \widetilde{E}_i^{'} \end{bmatrix} = P_j \begin{bmatrix} E_i \\ E_i^{'} \end{bmatrix} \tag{4.21}$$

The propagation matrix P is

$$P_j = \begin{bmatrix} e^{i\phi_j} & 0 \\ 0 & e^{-i\phi_j} \end{bmatrix} \tag{4.22}$$

For a multilayer structure, the relation between the forward (backward) electric fields of the first and the last (sth) interface is found to be

$$\begin{bmatrix} E_1 \\ E_1^{'} \end{bmatrix} = D_1^{-1} \left[\prod_{i=1}^{s} D_i P_i D_i^{-1}\right] D_s \begin{bmatrix} \widetilde{E}_s \\ \widetilde{E}_s^{'} \end{bmatrix} = \begin{bmatrix} M_{11} & M_{12} \\ M_{21} & M_{22} \end{bmatrix} \begin{bmatrix} \widetilde{E}_s^{'} \\ \widetilde{E}_s^{'} \end{bmatrix}. \tag{4.23}$$

Equation (14) also defines matrix elements M_{kl} where $k = 1, 2$, $l = 1, 2$.

The reflectivity coefficient r is given by the following equation:

$$r = \left[\frac{E_1^{'}}{E_1}\right]_{\widetilde{E}_s^{'}=0} = \frac{M_{21}}{M_{11}} \tag{4.24}$$

Finally, the reflectance R is obtained as

$$R = |r|^2 = \left|\frac{M_{21}}{M_{11}}\right|^2. \tag{4.25}$$

at the normal incidence and reflection of the beams $\cos\theta_i = 1$, by simplifying the dynamical matrices and making the dynamical matrices of the TE and TM waves to

be the same. A mulilayer is composed of many pairs of high n_H and low n_L refractive index media. The dynamical matrices for the high and low refractive index media become:

$$D_H = \begin{bmatrix} 1 & 1 \\ n_H & -n_H \end{bmatrix} \tag{4.26}$$

and

$$D_L = \begin{bmatrix} 1 & 1 \\ n_L & -n_L \end{bmatrix} \tag{4.27}$$

In designing a high reflectance multilayer, the thickness of each layer is chosen to be a quarter wavelength $d_i = \lambda/4$. Constructive interference ensures that the reflectance of the multilayer reaches the maximum. As result, the phase factor ϕ_i becomes $\pi/2$. The propagation matrix can be rewritten as

$$P = \begin{bmatrix} i & 0 \\ 0 & -i \end{bmatrix} \tag{4.28}$$

Finally, the reflectance R can be expressed in terms of n_0, n_H, n_L, and n_T as

$$R = \left[\frac{1 - \frac{n_T^2}{n_0} \left(\frac{n_H}{n_L} \right)^{2N}}{1 + \frac{n_T^2}{n_0} \left(\frac{n_H}{n_L} \right)^{2N}} \right]^2 \tag{4.29}$$

Where n_0 and n_T are the refractive indices of the media through which the electromagnetic wave is emitted (first medium) and transmitted (last medium), respectively. When the multilayer are stacked at quarter optical wavelength and with configuration

$n_{air}/H(LH)/n_s$ (n_s is the refractive index of the substrate), and for a fixed wavelength $\lambda = \lambda_o$ the reflectivity can be written as

$$R_o = \left[\frac{1 - \frac{n_H^2}{n_s} \left(\frac{n_H}{n_L} \right)^{2N}}{1 + \frac{n_H^2}{n_s} \left(\frac{n_H}{n_L} \right)^{2N}} \right]^2 \tag{4.30}$$

From the equation (4.30) one can see that high reflectivity and wide PBG can be obtained with large N and/or high ratio n_H/n_L.

For $N \geq 15$, $\frac{n_L}{n_H} << 1$ equation 4.30 becomes

$$R = 1 - 4\frac{n_s}{n_0} \left(\frac{n_L}{n_H} \right)^{2N}$$

Chapter 5

Experimental

5.1 Introduction

In order to fabricate a multilayer using organic polymers, the self-assembled properties of block copolymers and the co-extruded polymers have been studied to obtain periodic structures of refractive indices [65], [66], [67], [68]. Several methods have been used for fabrication of multilayer including self assembly method and co-extrusion method. The major weakness of these two methods is the difficulty in controlling the layer thickness. The co-extrusion method needed a high cost apparatus and complicated procedure. On the other hand the self assembly method uses block copolymers that can not be dye doped. A few papers demonstrated multilayer mirrors by the use of spin coating polymers [69]. However, high reflectivity at desired wavelength couldn't be obtained due to the following critical parameters:

- Low contrast of refractive indices of used polymers.
- Inaccurate control of the uniformity of layer thickness over the area of the

substrate.

- Inaccurate control of the overall thickness of each layer at the quarter wavelength optical thickness.

Among the multilayer fabrication methods described earlier, spin coating is the simplest and have the lowest cost. Photoresist have been coated on substrates using spinners for electrical and optical purposes. Then mechanisms of spin coating and characteristics of the coated films have been studied in detail[70], [71]. Nowadays, spin coating techniques are being industrially used for manufacturing of digital versatile disks [72], organic light emitting diodes [73], planar waveguides and insulators of large-scale integrated circuits [66].

The fabrication process and the obtained results of multilayered mirror by spin coating of organic polymers will be shown in following section.

5.2 Materials and methods

A high reflection multilayer mirror is fabricated by alternate stacking of a high- and a low-refractive index layer at quarter wavelength optical thickness. In order to achieve high reflection and wide band gap by stacking small number of layers of organic polymers, the selected two polymers in our experiment is based on the following points:

- The polymers should have relatively high refractive index ratio with low absorption and low scattering.

- The combination of the solutes and solvents; a solvent should only dissolve the

corresponding solute. Otherwise, penetration of the upper layer solvent to the lower layer will occur.

From the wide range of available polymers, two polymers were selected namely: poly(vinyl carbazole) (PVK) and poly(acrylic acid) (PAA), as high and low refractive index material, respectively. The PVK and PAA polymers have relatively high ratio of n_H/n_L and good transparency in a visible wavelength. Their molecular structures are shown in Fig 5.1, and their refractive indices are 1.683 for PVK and 1.420 for PAA at the Na D-line.

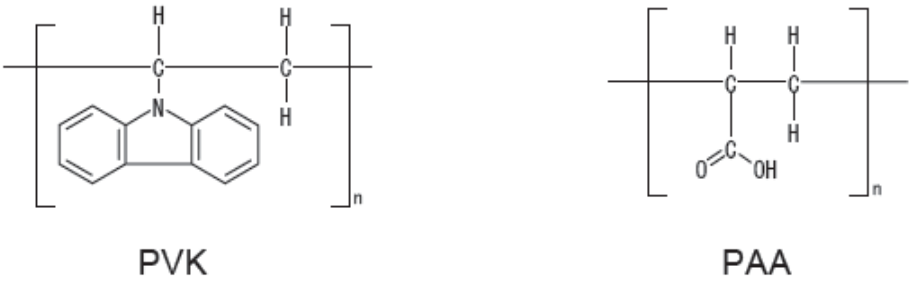

Figure 5.1: Shematic of molecular structure of PVK and PAA

Organic nonpolar solvents like toluene and chlorobenzene dissolve PVK, unlike polar solvents such as water, alcohols and esters which can dissolve PAA but not hydrocarbons. Therefore, chlorobenzene and water were selected as solvents for PVK and PAA, respectively.

PVK (powder, average Mw ≈1,100,000) and PAA (35wt% solution in water Mw≈250.000) were from Aldrich with high purity 99% and were used without any further purification. Because film thickness is highly affected by polymer's concentration and spin coater speed, polymer solutions at various concentrations were prepared. A single layer form each polymers at various concentrations was stacked on samples of glass substrate (2.5x2.5cm). Figure 5.2 shows a significant interaction between these two

factors. The average thickness of polymers decreases as spin angular velocity increases from 3000 rpm to 6000 rpm for both concentrations. But the layer thickness in the case of high polymer concentration was always higher compared to low concentrations for both polymers (Fig. 5.2). This is an important factor that has to be taken in consideration in the experimental procedure.

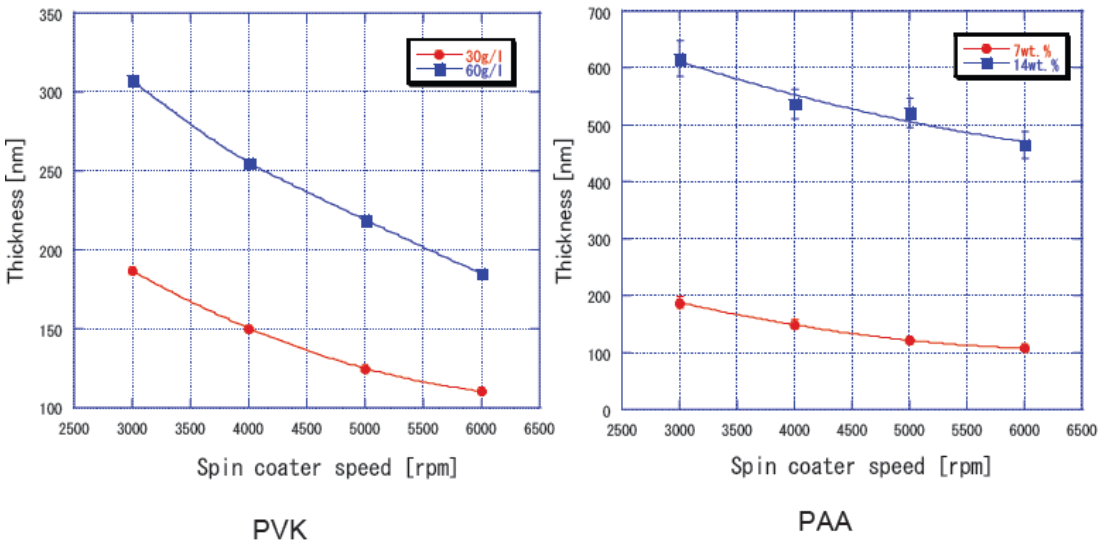

Figure 5.2: The effect of polymer concentration and rotating speed on the film thickness

Literature review showed that the minimum or maximum transmissivity of the single stacked depends on the refractive index of the stacked layer at the quarter wavelength multiplied by odd numbers. The quarter wavelength optical thicknesses can be controlled without knowing the exact values of refractive indices at specified wavelength. Selection of the odd numbers is possible by measurement the geometric thickness of layer using the scanning stylus.

For the fabrication of a multilayered mirror at specified wavelength of 632nm, the geometrical thickness of PVK and PAA were calculated using the refractive indices

at the Na D-line to be 99nm and 115nm which corresponding to a quarter wavelength optical thickness of 158nm. Figure 5.3 shows that the transmissivity of a single layer of PVK coated on the glass substrate was lowest at wavelength value around 632 nm. But the transmissivity of PAA single layer was maximum at the same wavelength value. This is because the refractive index of the glass substrate (1.52) is lower than that of PVK and higher than that of PAA. The minimum or maximum transmissivity were also obtained, when the optical thickness was equal to the quarter wavelength multiplied by an odd number. The geometrical thickness corresponding to the quarter wavelength can be found at the first step, since the half wavelength given by the difference of two adjacent odd numbers was much longer than 50nm. In the present case, the maximum or minimum wavelength corresponding to the quarter wavelength was set longer than the designed one. Then, the solutions concentrations were gradually reduced until the monitored wavelength at the maximum or minimum transmissivity approached the designed one within 10nm. After that the rotation speed of the spinner was adjusted until the minimum or maximum transmissivity values of the single coated layer appear at the designed wavelength within a few nanometers.

We fabricated a polymeric multilayered mirror designed at wavelength of 1064nm. The mirror was fabricated by poring, spin coating and baking of alternating PVK and PAA layers at a pre-designed rotation speed that produces an optical thickness with quarter wavelength of 1064nm. The solutions of PVK and PAA were prepared with 35% poly(acrylic acid) in water at a concentration of 30g/l and 7% by weight, respectively. The rotation speed was 3900 rpm for PVK and 3000 rpm for PAA. After coating one layer it was backed for 10 min. at a temperature of 80 degrees to dry the solvent. Mirrors with 11 stacked layers were manufactured and tested by comparing

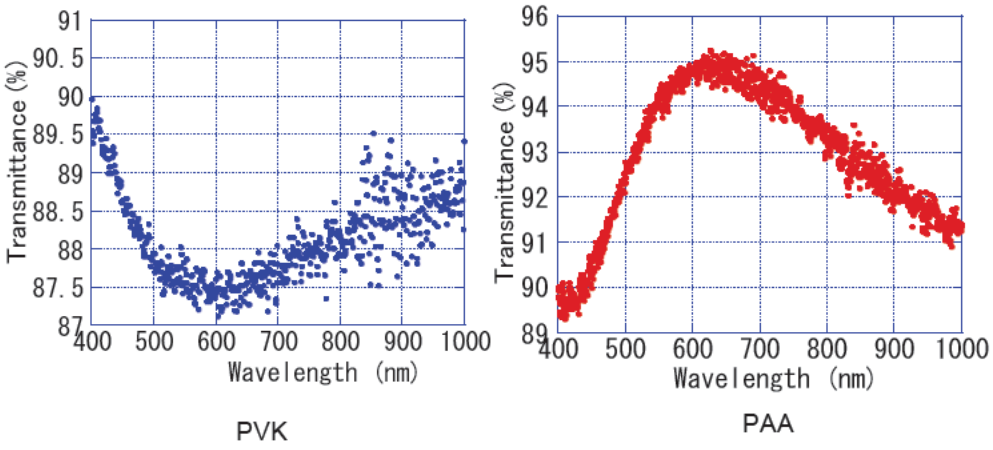

Figure 5.3: Transmittance of a single coated layer of PVK and PAA designed at 632nm

the experimental and theoretical reflection as shown in Figure 5.4. The maximum experimental reflection of the fabricated mirror was about half of the theoretical reflection.

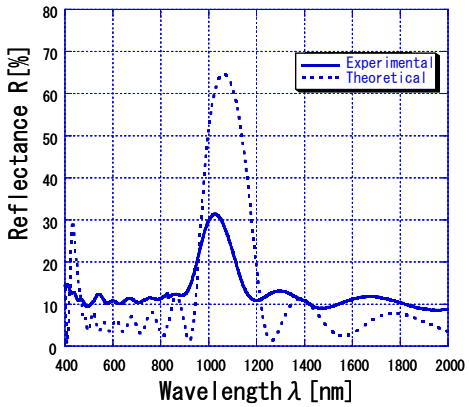

Figure 5.4: Experimental and theoretical reflectance of 11 layers

A microscopic image of the fabricated multilayer was taken to explain the large difference between experimental and theoretical reflection. As shown in Figure 5.5 a deterioration of the multilayer surface was found which could be probably attributed

to the penetration of one or both solvents from one layer to another.

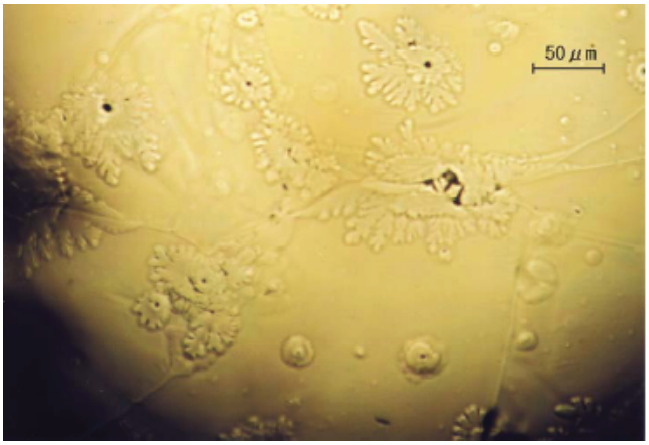

Figure 5.5: Microscopic image of the fabricated multilayer

Mixing of the solvents between layers was examined experimentally by poring various combination of polymers and solvents as illustrated in figure 5.6. Experimental results showed that poring chlorobenzene solvent on the layer of PAA stacked on the glass substrate or on a single layer of PVK (case II, III) had no effect on mirror degradation. Poring water on a layer of PVK (case I) had also no effect on sample deterioration. However, poring water on a stacked of a single layer of PAA above a layer of PVK caused a significant deterioration in the multilayer surface. Apparently water penetrates the PVK layer through the small molecular pores and dissolved PAA layer causing significant deterioration of the mirror layers.

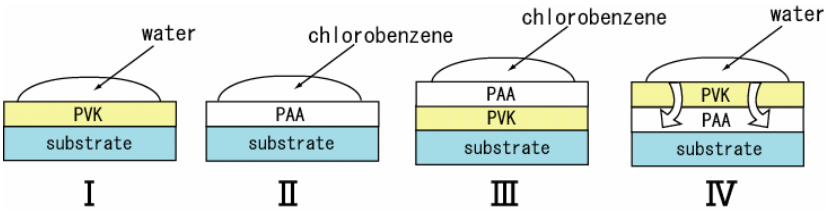

Figure 5.6: Verification experiement of the penetration

Experiments demonstrated that using low molecular-weight solvents like water is unsuitable for multilayer fabrication. Therefore, a high molecular weight solvent for PAA should be used in order to completely eliminate problems caused by water. A commercially available PAA in powder form was purchased from Aldrich having a molecular weight of about 2.000. A high molecular weight solvent, diacetone alcohol, was selected to prepare PAA solutions.

In order to prepare polymers solutions, specific quantities of PAA with diacetone alcohol and PVK with chlorobenzene were mixed together and stirred with magnetic agitator for 24 hours at normal room temperature. The PVK and PAA solutions were prepared at a concentration of 50 and 30g/l, respectively Using these two solutions, a polymeric multilayer mirror at wavelength of 1064nm was fabricated by spin coating and baking of layers. The rotation speed of the spin coater for the PVK and PAA determined from the thickness of the single layers on the glass substrate were 3200 and 2100 rpm, respectively.

Figure 5.7 represents the reflectance spectrum of a mirror designed at 1064nm wavelength and fabricated with various number of layers using simple process of stacking and backing. Baking was carried out at 80 degrees for 10 min. in order to evaporate the solvent. As shown in Figure 5.7 reflectance increased with the number of polymeric layers. However, maximum reflectivity seemed to occur at wavelengths different than the designed wavelength of 1064 nm and these deviations increased with the number of layers. This can be explained by the non uniformity of reflection distribution over the sample area caused by uneven thicknesses of various layers.

The spatial distribution of the reflectivity was measured by scanning a mirror area of 10x10 mm^2 using normally incident Nd:YAG laser. The experimental setup is shown in Figure 5.8.

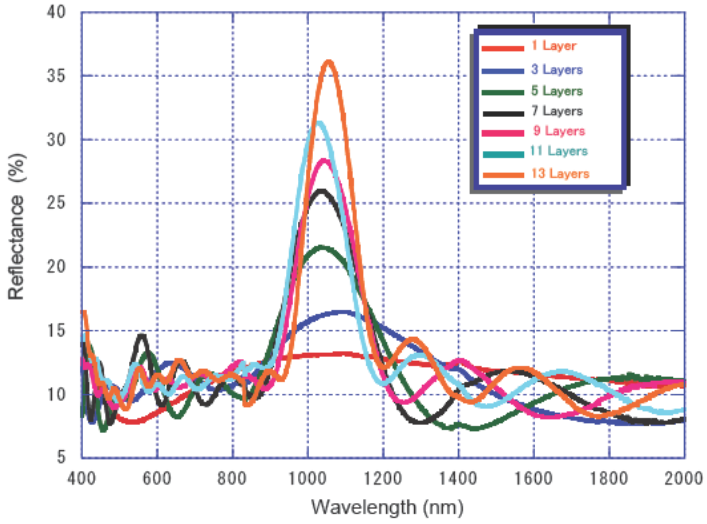

Figure 5.7: Reflectance spectra of variously stacked multilayer for 1064nm

Figure 5.9 shows the reflection percentage from different areas of the mirror. The wavelengths at reflection peaks shift to lower values compared to the designed wavelength in the center of the mirror, and to a higher values in the border. The variations occurred because the thickness of the multilayer was thinner in the center of the sample mirror compared to the border areas. The thickness variations were probably due to the influence of spin coater's strong vacuum.

Another mirror sample was prepared using a digital spin coater (Mikasa) and the reflection percentage from various areas of the mirror was measured. Figure 5.10 shows the reflections peaks from the center and edges of mirror occurred at approximately similar wavelengths indicating a uniform multilayer thickness. Apparently digital coating improved the thickness uniformity of the multilayer with thickness variations within few nanometer.

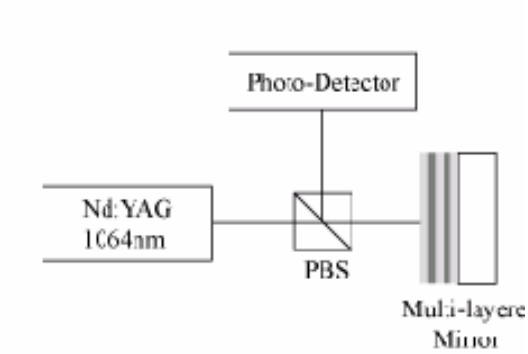

Figure 5.8: Experimental setup of the reflectivity spatial distribution

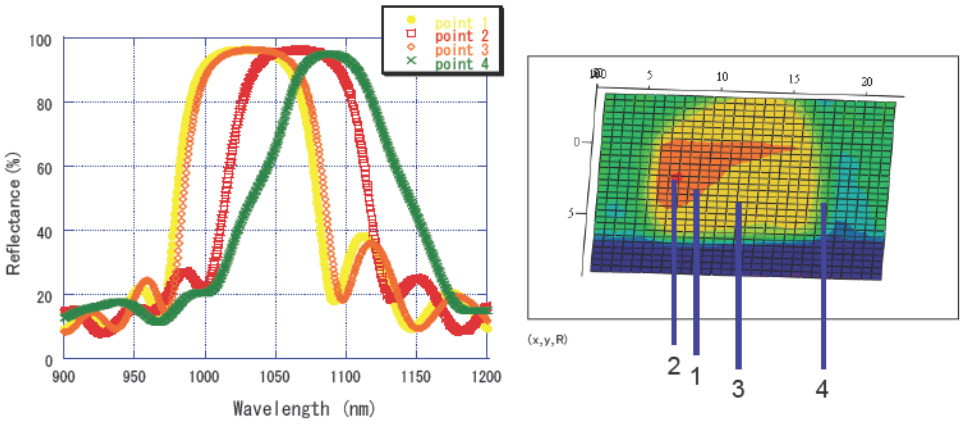

Figure 5.9: Experimental result of the reflection in different area of the sample

5.3 Results and discussion

Figure 5.11.shows the experimental transmission spectra obtained for a mirror designed at a wavelength of 1064 nm as affected by the number of layers. Increasing the number of layers through a simple repetitive process of spin coating and baking resulted in an increased mirror transmissivity at the designed wavelength. The peak transmissivity of 7 layers mirror was about 65% compared to only 5% for a 35 layers mirror. The peak wavelength of 1053nm for the 35 stacked layers indicates that the thickness deviation of each layer was only 2~3nm. The reflectivity at 1053nm was

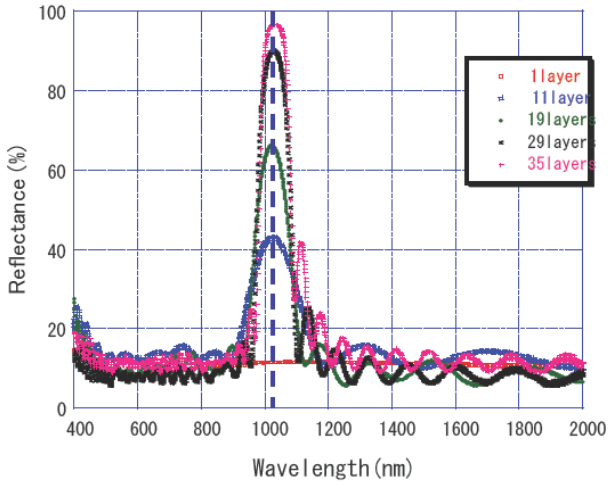

Figure 5.10: Reflection spectra of a polymeric multilayered mirror fabricated with digital spin coater

95.7%, whereas that at 1064nm was 95.3%.

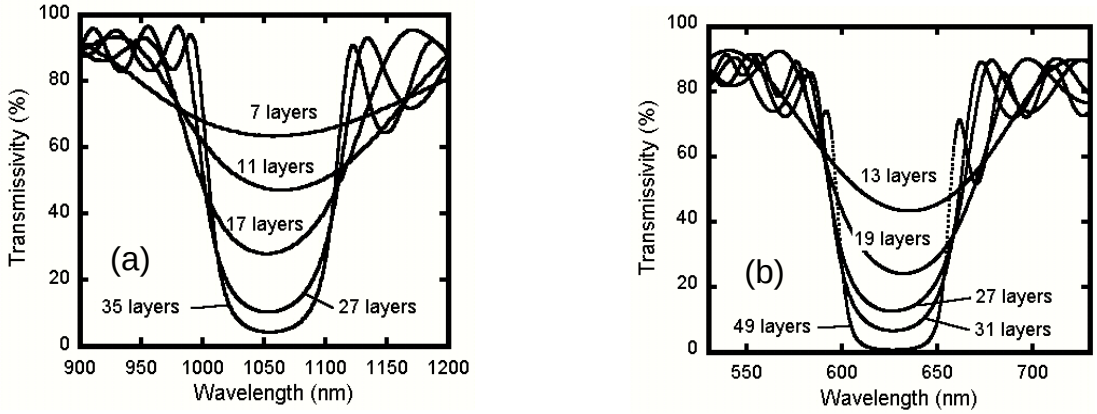

Figure 5.11: Transmission of polymeric multilayer (a): designed at 1064nm R=95.3%, (b): designed at 632nm R=99%.

A smaller designed wavelength value requires thinner multilayer. In this case, even the diacetone alcohol might penetrate the PVK layer thus deteriorating the multilayer. Nevertheless, attempts were successful in fabricating a multilayered mirror for a wavelength of 633nm. The transmissivity spectrum of a multilayer mirrors up to

49 stacked layers is shown in Figure 5.11. Experimental results showed that polymeric multilayers created high reflection up to 99% when the number of layers reached 45. The reflectivity values obtained in here were higher than that obtained by Alvarez et al [69]. These results indicated the proper selection of polymers-solvents combination and a good control over experimental conditions. Multilayer mirrors were produced at high accuracy with negligible thickness variations within few nanometer as shown in Figure 5.12 which displays the photographs of the mirror fabricated on the glass substrate with diameter of 30mm.

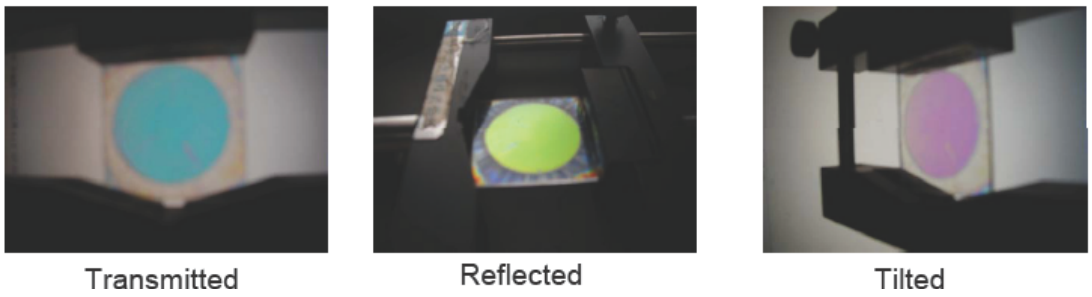

Figure 5.12: Photographs of a 45 layers stacked polymeric mirror fabricated on glass substrate

5.4 Conclusion

The polymeric multilayers have many advantages over conventional inorganic ones because its widely used for fabricating active or novel photonic devices. In addition polymers can be easily processed and variously functionalized by dye doping. We chose a combination of polymers and their solvent for fabricating a multilayered structure and controlled the thickness of each layer within few nanometers by spin coating. Reflectivity values higher than 95% at designed wavelength were achieved by stacking only 35 layers. Results also showed that high reflectivity could be obtained

by stacking layers of PVK dissolved in chlorobenzene and PAA dissolved in diacetone alcohol at quarter designed wavelength optical thickness.

The procedure of achieving the quarter wavelength optical thickness can be summarized as follow:

- The first step was to determine the approximate concentration of polymers that yielding an appropriate geometrical thicknesses. The thickness of the spin coated layer on the glass substrate was measured with the scanning stylus with high accuracy of around 30nm. The rotation speed of the spinner was set at 3000rpm in the consideration of the volatility of the solvents and the thickness of a hundred nanometers.

- The second step was to estimate and determine the concentration of the solutions that provided the quarter wavelength optical thickness. The optical thickness could be monitored using a spectrometer.

The use of digital spin coater improved the uniformity of the surface. Industrial application of Polymeric multilayer doped with functional dye, fabricated by spin coating, will produce various active devices for industrial application. We can control the intensity of the transmitted monochromatic light by changing the refractive index and/or the optical thickness by applying an electric field or by irradiating a lightwave. The fabrication process and results of electro-optic device and all optical device will be shown in the following part of the thesis.

Part II

Applications

Chapter 6

Introduction

With the advance of the information-communication society, it is easy to predict that the volume of communications will increase. This will inevitably be accompanied by a growing number of communication-network devices and a corresponding demand for improved device performance. When developing new devices, it is thus important to focus on increasing speed while reducing power consumption, size, and price.

Multilayers are expected to play an important role in the development of new optical devices [74], [75]. they can be used as passive devices such as simple waveguides, arrayed waveguide gratings, Bragg gratings, thin film filters, and microring resonator filters. The device possibilities for multilayer will be greatly enhanced by the addition of optical nonlinearities; such possibilities include ultrafast all-optical switching and light modulation for communications, and potentially even optical computing [76], [78], [79], [80], [81], [82]. Correspondingly, the influence of the photonic bandgap can be exploited to enhance or modify the behavior of nonlinear optical materials. For example, the flattening of the photon dispersion relation near a photonic bandgap has been demonstrated to ease phase-matching constraints leading to enhance second- and

third-harmonic generation [83], [84] and localization associated with defects has been shown to enhance a variety of third-order nonlinear processes in periodic multilayer [85], [86], [87], [88], [89].

With several important recent advances, polymers are fast becoming important materials for optoelectronics. Significant examples include mechanically flexible "electronic paper" [90] and high efficiency light-emitting diodes based on electroluminescent conjugated polymers [91]. Similar promise is being presented for polymers in telecommunications-related integrated optical devices due to several favorable material features [92]. For instance, as required by the application, polymer materials can be made functional in several ways. Otherwise passive polymers that are not intrinsically functional can be doped with numerous optically active dopants such as organic laser dyes [93], rare-earth light-amplifying complexes [94], or electro-optic chromophores [95].

In this part of the thesis we will show the fabrication process and the obtained results of the electro-optic and all optical devices. Such devices are fabricated by use of 2^{nd} and 3^{rd} order nonlinear chromophores doped polymeric multilayer.

Chapter 7

Background

7.1 Light propagation through nonlinear media

Ordinary light sources have rather low intensity and interact with matter linearly. The creation of lasers in the 1960's gave birth to a new area in optics "nonlinear optics" by opening the possibilities to observe and manipulate the nonlinear effects. The nonlinear effects can be classified by the order of nonlinearity they exhibit.

A light wave consists of two components: electric and magnetic fields. These fields oscillate sinusoidally with high frequencies. Interaction of light and matter results in some displacement of the charge distribution inside the atoms or molecules of the material. The atoms, constructing the material, are seen as charge distributions pushed away from their equilibrium state when exposed to the electric or the electromagnetic field.

When the field is weak light interacts linearly with the matter. In the case of high intensity of the light, electromagnetic field modifies the optical properties of the medium strongly, which effects the propagation of the radiation. Broadly speaking,

nonlinear matter is a medium whose optical response depends on the intensity of the optical field that propagates through it. One of the typical nonlinearties is the change of the dielectric constant due to the Pockel or Kerr effect. The second and third order nonlinearities enrich optics in general, and, in particular, the light propagation through nonlinear photonic crystals [96]. Nonlinear photonic crystals were successfully applied in the field of the frequency mixing and harmonic generation [97], [98], efficient phase matching of several wavelengths [99], as optical diodes [100] optical switchers and limiters [101] to mention just a few examples.

Nowadays a lot of nonlinear effects are discovered and studied in different materials (gases, liquids and solids). The area of applications of these nonlinear phenomena is vast. They are applied in medicine, biology, telecommunications, military and industrial applications. One can mention a few of them, like, nonlinear photo-absorption, harmonic generation, self-focusing, nonlinear photo ionization and dissociation, phase conjugation, etc. There are two all-optical switching qualitatively different nonlinear interactions. The first one occurs when the light frequency is close to a resonant frequency of the media. In this case nonlinear effects appear at rather small intensities (W/cm^2). The nonlinear optical effects are accompanied in this case by undesirable strong photo-absorption. To avoid absorption, one can induce nonlinearity by a nonresonant field. However, higher intensities are demanded in that case.

7.2 Nonlinearity theory

The presence of an electric field $E(t)$ in a dielectric material causes a displacement of the electric charges inside the medium. The induced dipole moment per unit volume is defined as the polarization $P(t)$, which can be expanded as a power series in the

applied electric field:

$$P_i = \varepsilon_0(\chi_{ij}^{(1)} E_j + \chi_{ijk}^{(2)} E_j E_k + \chi_{ijkl}^{(3)} E_j E_k E_l + \cdots) \tag{7.1}$$

Where $\chi^{(n)}$ is the n^{th} order electric susceptibility and a tensor of rank $(n+1)$. All susceptibilities of order n=2 and higher are responsible for nonlinear optical effects. Linear optics is described by $\chi^{(1)} = \varepsilon_r - 1$, where ε_r is the relative dielectric permittivity or dielectric constant.

Second-order effects that are dependent on the first hyperpolarizability tensor term $\chi^{(2)}$ and third-order effect that are dependent on the second hyperpolarizability tensor term $\chi^{(3)}$; other higher order effects are difficult to observe.

For a medium to exhibit second-order nonlinear susceptibility it should not possess a center of symmetry, i.e. it should be noncentrosymmetric. All media and molecules exhibit third-order response. Basically all forms of matter exhibit nonlinear optical phenomena. But to be useful in a device, the material must exhibit a high degree of nonlinearity at a reasonable power level.

Many of the interesting phenomena of nonlinear optics derive their behavior from the nonlinear index of refraction. It has led to a variety of fascinating applications. The general dependence of the nonlinear refractive index on intensity can be expressed as:

$$n = n_0 + \Delta n \tag{7.2}$$

The change in the refractive index Δn over its value at low intensities n_0 depends on the applied voltage (Pokel effect) or the control beam (Kerr effect). This dependence is made more explicit in the following chapters.

The nonlinear index coefficient is related to the second order (linear electro-optic or Pockel effect) or third order (Kerr effect) nonlinear susceptibility that appears in the expansion to second or third order, respectively, of the nonlinear polarization as follow:

2^{nd} order:

$$P_i^{(2)}(\omega) = 2\varepsilon_0 \sum_{jk} \chi_{ijk}^{(2)} E_j(\omega) E_k(0) \tag{7.3}$$

3^{rd} order:

$$P_i^{(3)}(\omega) = \frac{3}{4}\varepsilon_0 \sum_{jkl} \chi_{ijkl}^{(3)} E_j(\omega) E_k(0) E_l(0) \tag{7.4}$$

While the linear effect has been known since 1906, 3^{rd} order nonlinear Kerr effect was not observed until the invention of the laser in 1961 [101], [102]. It was the availability of high intensity coherent light sources that lead to various experiments related to the change of material's properties by the presence of light. The invention of the laser thus effectively marks the starting point of nonlinear optics [103].

Chapter 8

Electro-optic Device

8.1 Introduction

From the fundamental materials viewpoint, the electro-optic (E-O) effect is due to the change in optical susceptibility caused by molecular, ionic, and electronic polarization as a result of an applied electric field.

Usually the change in the refractive index is very small. Nevertheless, its effect on the optical wave propagation can be very high. For example if the refractive index increases by 10^{-5}, an optical wave propagating a distance of 10^5 wavelengths will be subjected to an additional phase shift 2π . E-O effect can be used for optical communication and optical signal-processing applications, by applying an electric field to change the refractive index, the spatial and temporal distribution of the light waves traveling in an E-O medium will be also changed as indicated by the following examples:

- A tunable lens whose focal length can be changed by refractive index change.

- A prism whose beam deflection ability is controllable can be used as an optical scanning device
- Optical phase modulator in which light transmitted through a transparent plate of controllable refractive index undergoes a controllable phase shift.
- Wave retarder which can be used to change the polarization properties of light.
- Optical intensity modulator or optical switch.

8.2 Fundamental theory

A polymer doped with 2^{nd} order nonlinear chromophore and poled in the direction of the normal surface, its electro-optic tensor can be expressed as:

$$\begin{vmatrix} 0 & 0 & r_{13} \\ 0 & 0 & r_{13} \\ 0 & 0 & r_{33} \\ 0 & r_{13} & 0 \\ r_{13} & 0 & 0 \\ 0 & 0 & 0 \end{vmatrix}$$

where r_{33}=3r_{13}.

A 2^{nd} order nonlinear dye doped at least one of the polymers constructing the multilayered mirror (Fig. 8.1), can be used as an electro-optic device.

For an electric field in the direction of the surface normal (Z-direction), the refractive index of the doped layers is ellipsoid and described by :

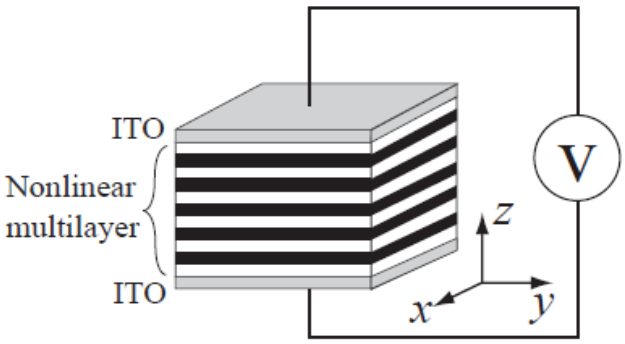

Figure 8.1: Electro-optic device illustration

$$\left(\frac{1}{n_0^2} + r_{13}E_z\right)(X^2 + Y^2) + \left(\frac{1}{n_e^2} + r_{33}E_z\right)Z^2 = 0 \tag{8.1}$$

where X, Y and Z refer to the principal dielectric axes of the electro-optic device (Fig. 8.1), n_o is the ordinary refractive index, and n_e is the extraordinary refractive index.

When an electric field is applied in the Z direction and a polarization of propagating light is X or Y direction, the change in the refractive index due to Pockel effect is:

$$\Delta n_o = -\frac{1}{2}n_o^3 r_{13}E_z = -\frac{1}{2}n_0^3 r_{13}\frac{V}{l} \tag{8.2}$$

where (V) is the modulation voltage and l is the separation distance between the two indium tin oxide (ITO) electrodes. This induced Δn_0 changes the device transfer characteristics by the phase change.

8.3 Device structure and operation principle

An electro-optic device can be fabricated by two different multilayer configurations. The first configuration is a dielectric multilayer structure without a defect as displayed in Figure 8.2(a), and the second configuration is a stack of a dielectric multilayer structure with a defect layer (Fig 8.2(b)) called Fabry-Perot cavity type. The operational wavelength of the electro-optic device can be either at the band edge (multilayer without defect) or at the defect peak (multilayer with defect).

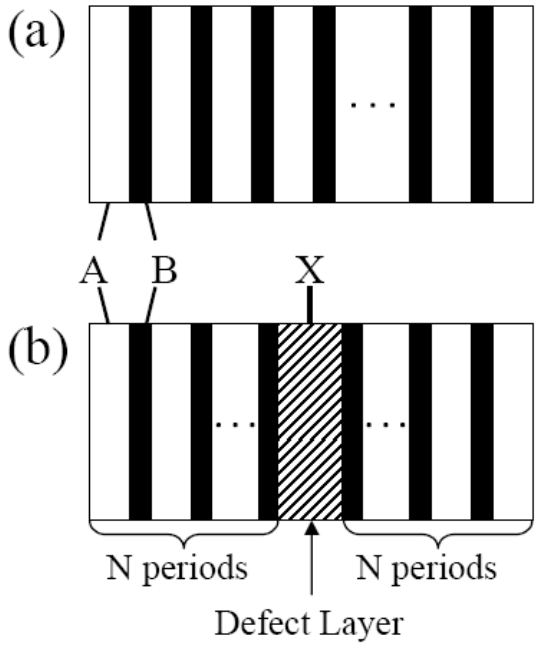

Figure 8.2: Model of dielectric multilayer structures without defects (a) and with a defect (b)

The origin of the nonlinear enhancement in both configurations can be understood from Figure 8.3 and Figure 8.4, which depict the calculated steady-state electric field amplitude (normalized to input) within a multilayer sample at both the defect mode wavelength and a wavelength near the band edge. Although the amplitude at the

output is approximately equal, the field within the defect layer is much larger at the defect mode.

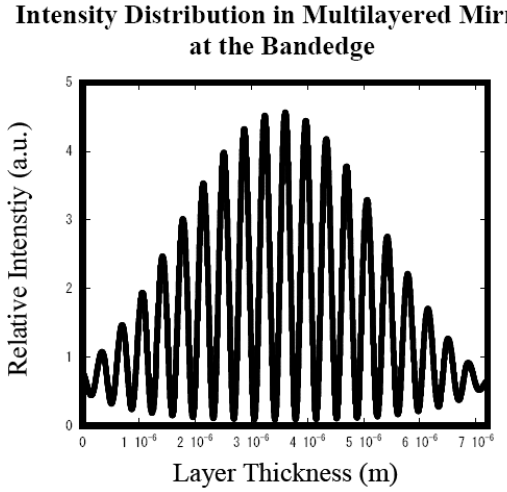

Figure 8.3: Calculated electric field intensity distribution within perfect multilayer structure.

The field is enhanced near the defect layer so the effective nonlinearity is potentially larger, leading to a lower tuning threshold. But, the manufacturing requirement is very stringent because the defect peak depends largely on the reflectivity and the parallelism of the two mirrors. Also, the thickness of a defect layer must be kept within a tight range to keep defect at the designed wavelength. But this is not crucial for a device based on the shifting of the band edge. as long as the operational wavelength of the device is at the band edge.

In the present experiment we used the perfect multilayered mirror doped with 2nd order nonlinear dye. The fabrication process and the results are shown in the following section.

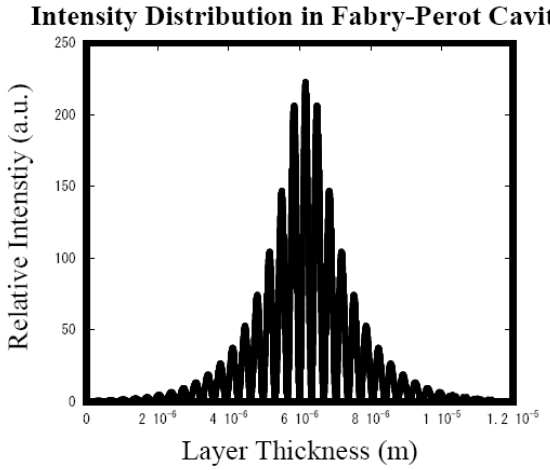

Figure 8.4: Calculated electric field intensity distribution within defect multilayer structure.

8.4 Fabrication

A multilayer mirror was fabricated by spin coating using PVK as the high refractive index layer and NLO disperse red1 (DR1) doped PAA as the low refractive index layer. The structure of the device is shown in Figure 8.5. The multilayer was designed at 1080nm In order to obtain a wavelength of 1064nm at the band edge. The calculated thickness of high and low refractive index layers were 161.42 nm and 190.14 nm, respectively.

This multilayer was sandwiched between two indium thin oxide (ITO) glasses as shown in Fig.8.5 with 0.1wt% of DR1 to enhance the electro-optic effect without high absorption. Then specific quantities of DR1 and PAA with diacetone alcohol and PVK with chlorobenzene were mixed together and stirred with magnetic agitator for 24 hours at normal room temperature. Using these two solutions, a nonlinear polymeric multilayer mirror at wavelength of 1080nm was fabricated by spin coating and baking of layers. The rotation speed of the spin coater for the PVK and DR1

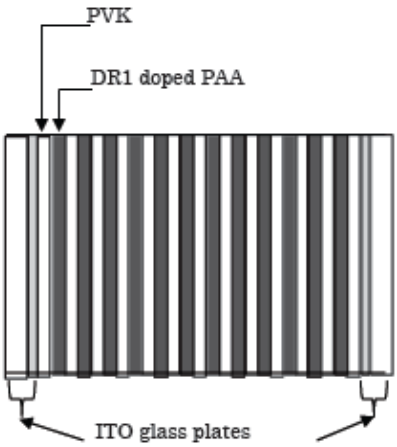

Figure 8.5: Sample structure consisting of PVK as high layer and DR1 doped PAA as low layer

doped PAA, determined from the thickness of the single layers on the ITO glass substrate, were 3400 and 2400 rpm, respectively.

The transmission spectrum of the fabricated device is shown in Fig. 8.6. Corona-discharge poling was performed on the multilayer to align the NLO chromophores with an applied voltage of 7 kV for 10 min. at the PAA glass transition temperature T_g of $110°C$ for the macroscopic second-order optical nonlinearity.

8.5 Measurement results and discussion

The intensity of monochromatic light can be controlled by changing the refractive index of the polymer in an electric field. Fig. 8.7 shows the effect of voltage on the transmission spectrum when the number of stacked layers is 39 layer. Applying high voltage of 140V/μm resulting in high shifting of the band edge. However, applied voltage larger than 100V/μm highly caused a dielectric breakdown.

We studied switching of the device using a setup shown in Fig. 8.8. Nd:YAG laser

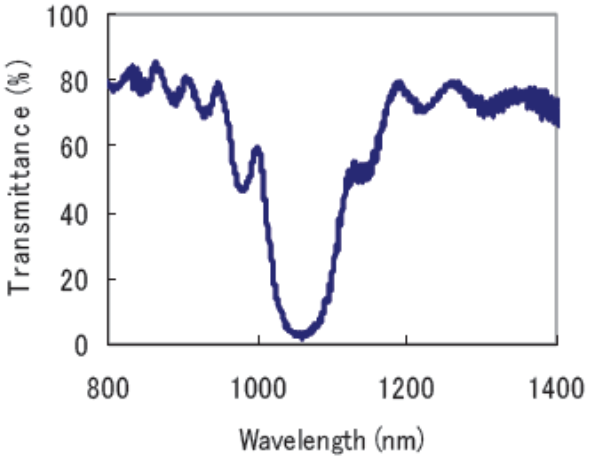

Figure 8.6: Transmittance of fabricated polymeric multilayer at designed wavelength of 1080nm

at 1064nm was irradiating the sample when a voltage of 100V/μm was generated by the pulse generator.

Fig 8.9 shows the temporal behavior of the transmission. The transmittance at zero voltage was about 10% for the CW operation of Nd:YAG laser. This is the "off" state of the device. When a voltage of 100V/μm was applied, the transmission reached 40% in microsecond order. This is the "on" state. The optical loss of higher than 50% was attributed to the absorption of ITO glass. From this change of the transmittance, the change Δn of the refractive index of the PAA layers was calculated to be 0.003, corresponding to $\simeq$20pm/V of the electro-optic coefficient of the DR1-doped PAA.

Electro-optic devices using a perfect multilayer type can be fabricated also by stacking layers at three quarter wavelength optical thickness. Figure 8.10 displays the calculated transmittance of staked layer at $\lambda/4$ and $3\lambda/4$ optical thickness. It shows that $\lambda/4$ stacks give wider band gap than the $3\lambda/4$ stacks, this latter has sharper band edge. The sharp band edge can be used to improve the transmission efficiency of the device. However, it's difficult to adjust the designed wavelength at

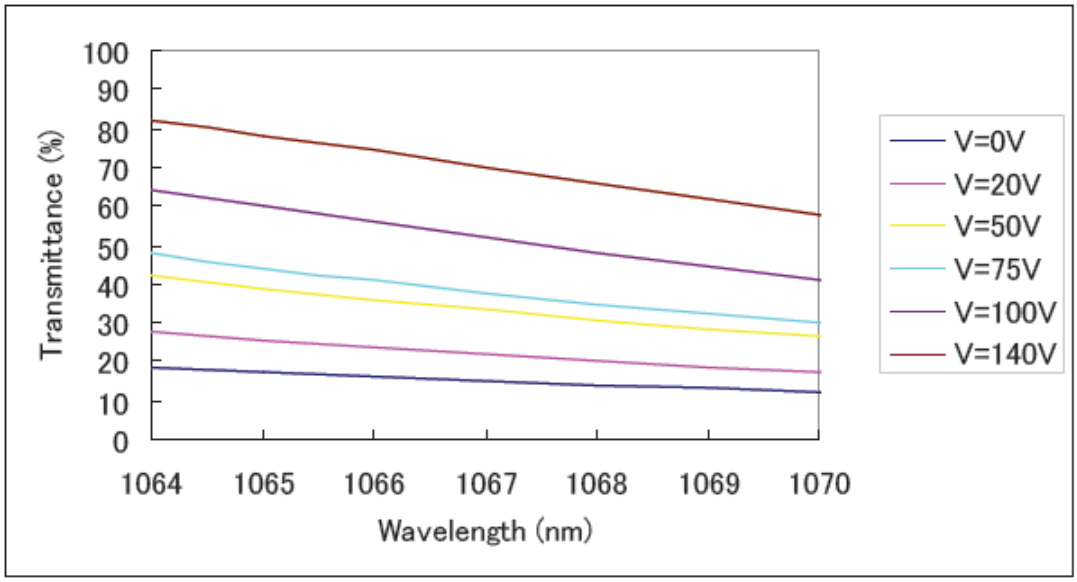

Figure 8.7: Band edge shifting dependance on applied voltage

sharp band edge.

8.6 Conclusion

We realized an electro-optic device operating at 1064 nm, by simply spin coating and baking alternatively PVK as high refractive index and DR1 doped PAA as low refractive index at quarter wavelength optical thickness. Transmission efficiency of 30% was achieved using this device as a switch by applying a voltage of 100V/μm.

Polymeric multilayer electro-optic devices can be used in future communication applications where a weight is an issue, compactness is a key, and the production cost is a critical factor like waveguide EO modulators, switches, laser diodes, and EO displays. They can also be used in integrated optics to increase the functionality.

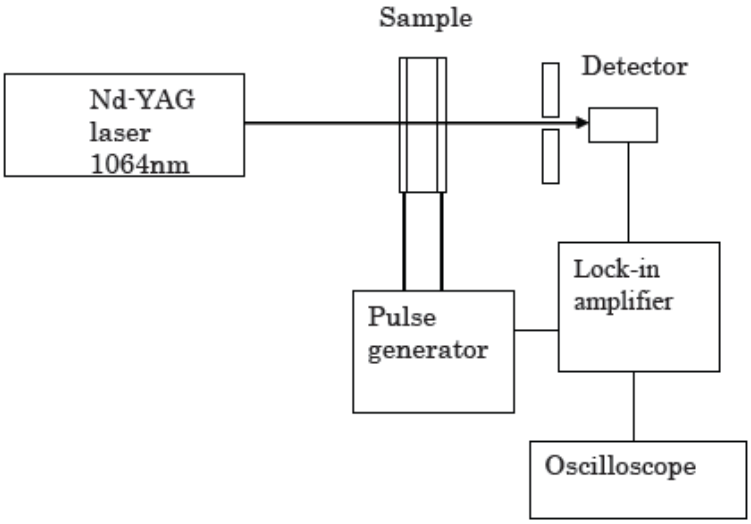

Figure 8.8: Experimenatl setup

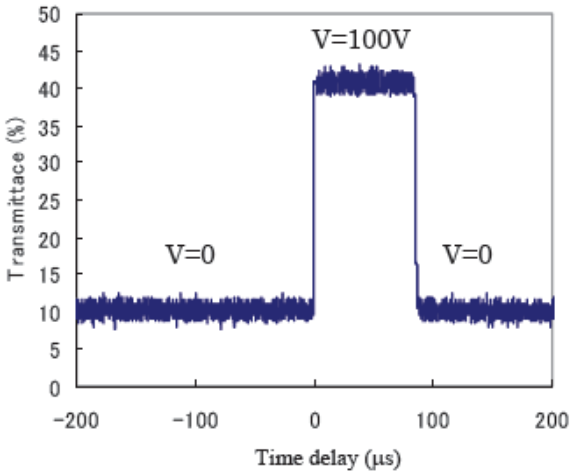

Figure 8.9: Transmittance intensity at V=0 and V= 100V

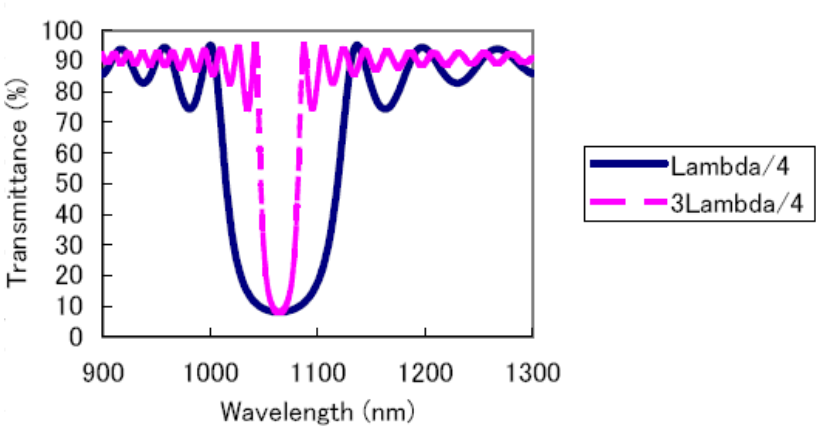

Figure 8.10: Transmittance spectrum of periodic multilayered mirror staked at quarter wavelength optical thickness and at three quarter wavelength optical wavelength.

Chapter 9

All-optical Devices

9.1 Introduction

Devices for all optical processing exploit ultra-fast nonlinear effects to control light with light. This means that an optical control signal selectively changes the properties of a nonlinear medium through the third order optical nonlinearity known as Kerr medium. The advantage of the all optical devices is the tremendous speed benefit compared to electronic solutions.

Organic materials, especially doped polymers, are known with fast response speed compared with other materials like semiconductors. However they possess low third order nonlinear susceptibility $\chi^{(3)}$. Using a third-order nonlinear choromophres-doped polymers for fabrication of the multilayer can increase the effective $\chi^{(3)}$ through the optical confinement.

In this chapter, $\chi^{(3)}$ dye doped polymers used for the fabrication of multilayer shows Kerr effect, When the refractive indices of the polymers change, the band structure of the multilayer also changes. Using this property, the nonlinear multilayer

can be used as all-optical device [76],[77],[79],[104].

9.2 Theory and device operation principle

Kerr nonlinear materials change their refractive index n_{NL} depending on light intensity inside the material:

$$n_{NL}^2(r) = \varepsilon_{NL}(r) = \varepsilon + \chi^{(3)} I(r), \tag{9.1}$$

where $I(r)$ describes the local intensity distribution and $\chi^{(3)}$ is the Kerr-coefficient of the nonlinear material and defined as:

$$\chi^{(3)} = \frac{n\Delta n}{12\pi} \tag{9.2}$$

We consider a mulitlayer, stacked as Fabry-Perot cavity type, containing a nonlinear isotropic Kerr polymers as shown in Fig. 9.1.

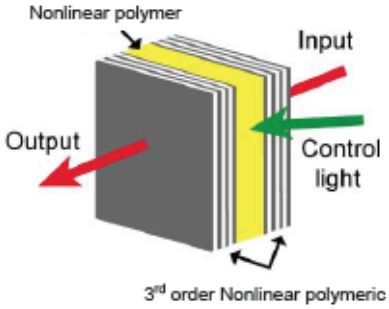

Figure 9.1: Polymeric multilayer stacked as Fabry-perot cavity type

The transmittance efficiency of a probe beam irradiating the Fabry-Perot cavity type multilayer at normal incidence is described by:

$$\frac{I}{I_0} = \frac{(1-R)^2}{(1-R)^2 + 4R\sin^2(\delta/2)} \tag{9.3}$$

with I_0 and I are the intensities of the incident and transmitted beam, respectively, R is the mirror reflectivity, $\delta = \frac{2\pi nl}{\lambda} + \varphi$ is the phase shift, l is thickness of the spacer, n is the spacer refractive index, and φ is the phase shift induced by the mirrors.

It is well known from the literature that the maximum peaks appear when:

$$\frac{2\pi nl}{\lambda} + \varphi = m\pi \tag{9.4}$$

with m is an integer.

Using a $\chi^{(3)}$ nonlinear dye doped polymer for the fabrication of multilayer as Fabry-Perot cavity designed to operate at the wavelength λ_1 , shows a maximum transmission of the wavelength at the defect peak as predicted by equation 9.4.

When control beam with a wavelength near the resonance of the dye (to avoid a maximum absorption), is incident on the multilayer, the maximum transmission at the defect peaks appear at another wavelength due to Kerr effect, and Eq. 9.4 is not satisfied for λ_1 and become:

$$\frac{2\pi(nl + \Delta nl)}{\lambda_1} + \varphi \neq m\pi \tag{9.5}$$

with Δnl is the total path length change.

The principle can be used as all optical devices. The fabrication process and results are shown in the next section.

9.3 Fabrication

The light intensity dependent change of the refractive index through the third-order optical non-linearity can be used for all optical devices. We fabricated a Fabry-Perot cavity type multilayer by using the third-order NLO styryl 9M, which possesses a large third-order NLO susceptibility $\chi^{(3)}$ with fast response [105].

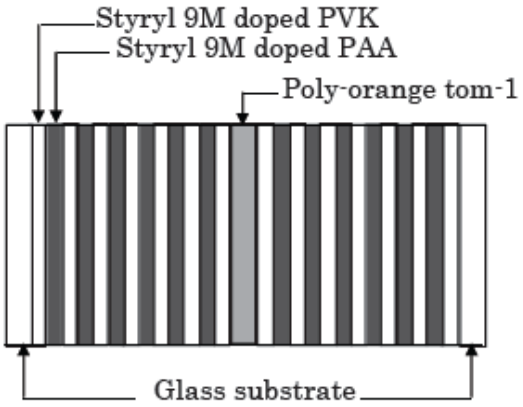

Figure 9.2: Ilustration of fabry-perot cavity type using Styryl 9M doped PVK and PAA as mirrors and Poly-orange tom-1 as spacer

The samples used in this experiment consisted of a pair of dielectric quarter-wave stacks surrounding a poly-orange tom-1 isophoronedisocyanate [106] defect layer. The quarter-wave stacks were fabricated by spin coating and backing alternatively a 3^{rd} order nonlinear dye doped polymers each was comprised of 17 periods of alternating Styryll 9M doped PVK and Styryl 9M doped PAA with optical thickness of 1064nm/4. The defect layer was created by spin-coating a poly-orange tom-1 solution, with optical thickness of 1064nm/2, onto a pair of the quarter-wave stacks and squeezing them together in a vise (Fig 9.2). A transmission scan from the sample is shown in Fig. 9.3.

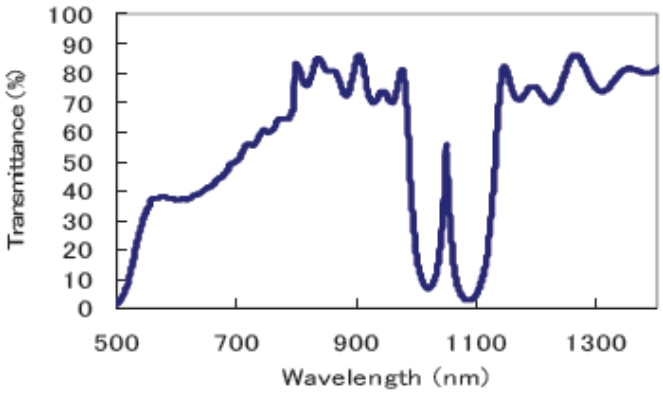

Figure 9.3: Transmittance of fabry-perot cavity

9.4 Measurement results and discussion

Fig. 9.3 shows that the defect peak in transmittance spectrum was at 1050nm, obtained for normal incidence using spectrometer. There were no transmission peak at a wavelength of 1064nm of the Nd:YAG laser. Then, we adjusted the peak to the proper wavelength by tuning the incidence angle.

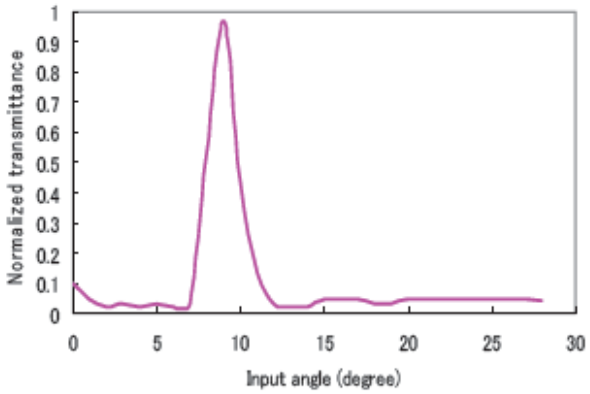

Figure 9.4: Angular tuning

Fig. 9.4 shows the angular dependence of the normalized transmission intensity for a wavelength of 1064nm. The transmittance reaches its maximum at 9°.

For confirmation of optical switching, we adopted the pump-probe method shown in Fig. 9.5. A CW Nd:YAG laser oscillated at 1064nm was used as a probe laser and was made incident at 9° to the normal of the sample surface. A second-harmonic of 532nm of a Q-switched Nd:YAG laser with a pulse duration and a pulse repetition of 100ns and 1kHz, respectively, was used as a control laser and was made incident at an angle of 30° from the probe laser.

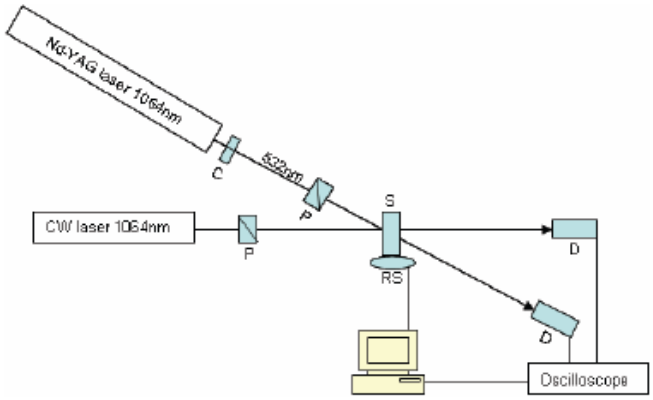

Figure 9.5: Experimental setup, P: polarizer, S: sample, RS: rotating stage, D: detector

Fig. 9.6 shows the probe-light transmittance. When the pulsed pump-laser was incident, the transmittance clearly changed. Due to the pump-induced shift of the photonic gap, the transmittance of the probe light reached its minimum of 10% for the peak of the laser pulse and then, it returned to the original value of 54% for the end of the laser pulse.

This optical switching of "on" and "off" was attained by using a 3 kW/cm^2 pump light. From the transmittance change of more than 40%, the third-order susceptibilities of the Styryl 9M-doped PAA and PVK were 302 and 351 m^2/V^2, respectively.

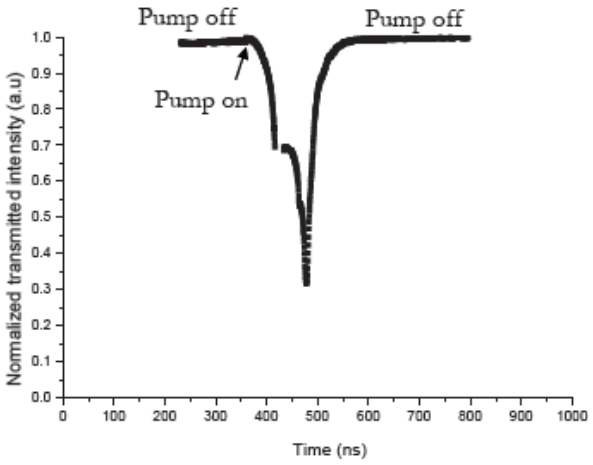

Figure 9.6: Response of the optical switch with the pump laser (pulse duration 100ns, pulse repetition rate 1kHz)

9.5 Conclusion

An all-optical device was fabricated by doping a high 3^{rd} order nonlinear dye styryl 9M in both layers, PVK and PAA, constructing the multilayer, and a poly-orange tom-1 was used as a defect layer. The device was confirmed as an optical switch, showing the transmission change of 44% by use of 3kW/cm^2 control beam.

Some of potential applications of this device for future communication such as power limiting, all-optical logic gating, VLSI compatible switching devices. Using these all-optical devices we can expect various applications in information storage, optical signal processing operations, and many other important applications.

Chapter 10

Summary and Recommendation for Future Works

The volume of communications is increasing due to the advancement of the society. This will inevitably be accompanied by a growing number of communication-network devices and a corresponding demand for improved device performance. Newly developed devices should have high speed capability, low price and low power consumption.

We succeed in the fabrication of multilayer mirrors by spin-coating of high refractive index ratio polymers. A multilayer is formed by stacking a high and low refractive index layers alternatively. Two polymers, poly(vinyl carbazole) and poly(acrylic acid) dissolved in chlorobenzene and diacetone alcohol, respectively, were used as a high and a low refractive-index layers. Optical thickness of layers at $\lambda/4$ was well controlled by adjusting the concentration of solutions and by changing the rotation speed of spin-coater. Experimental results revealed an increasing reflectivity with an increase in the number of layers through a repetitive process of spin-coating and solvent drying. Reflectivity more than 95% was observed at designed wavelength of 1064 nm by

stacking only 35 layers.

As an applications we fabricated an electro-optic and an all-optical devices by doping a polymeric multilayer with a second and third order nonlinear dye. The electro-optic device, operating at 1064nm was manufactured by simple spin coating and baking of alternatively PVK as high refractive index and DR1 doped PAA as low refractive index at quarter wavelength optical thickness. Transmission changes about 30% was achieved using this device as a switch by applying a voltage of 100V/μm.

The all-optical device operating at 1064nm was fabricated by doping 3rd order nonlinear Styryl 9M in both layers, PVK and PAA, constructing the multilayer, with an optical thickness of $\lambda/4$, and a poly-orange tom-1 was used as a defect layer, satcked with $\lambda/2$ optical thickness. The device was confirmed as an optical switch, showing the transmission changes of 44% by use of 3kW/cm^2 pump beam.

This research can be considered as a corner stone for future works. Further improvement to the current research can be done to fabricate an electro-optic and all-optical devices by the use of high nonlinearity chromophores, so the devices can be controlled with lower electric field and lower intensity of control beam. More investigation is needed to improve the speed of the all-optical device using femtosecond laser as control beam. In addition future investigations are necessary to illustrate bistability in all optical device.

Bibliography

[1] J. Bardeen and W. H. Brattain, Phys. Rev. 74, 230 (1948).

[2] W. Shockley, Bell Syst.Tech. J. 28, 435 (1949).

[3] L. R. Dalton, Pure and Appl. Chem., 76, 1421-33 (2004)

[4] H. Ma, S. Liu, J. Luo, S. Suresh, L. Liu, S.H. Kang, M. Haller, T. Sassa, L.R. Dalton, A.K.-Y. Jen, Advanced Functional Materials, 12, 565 (2002)

[5] Williams DJ, Angew Chem Int Ed Engl 23, 690 (1984)

[6] Meredith GR, van Dusen JG, Williams DJ, Amer. Chem. Soc. 233, 109 (1983)

[7] Garito AF, Singer KD, Teng CC, Amer. Chem. Soc. 233, 1 (1983)

[8] Moehlmann GR, Horsthuis WH, van der Vorst CP, Donach AM, Copeland JM, Duchet C, Fabre P, Diemeer MB, Trommel ES, Suyten FM, van Daele P, van Tomme E, Baets RG,.Proc SPIE 1147, 245 (1990)

[9] L. Eldada, "Photonic integrated circuits," in Encyclopedia of Optical Engineering, Ed. R. Driggers, Marcel Dekker, New York (2003).

[10] Meredith GR, Van Dusen JG, Wiiliams DJ, Macromolecules 15, 1385 (1982)

[11] H. Ghiradella, Appl. Opt. 30, 3492 (1991).

[12] E. Yablonovitch, Phys. Rev. Lett. 58, 2059 (1987).

[13] S. John, Phys. Rev. Lett. 58, 2486 (1987).

[14] E. Yablonovitch and T. J. Gitter, Phys. Rev. Lett. 63, 1950 (1989).

[15] K. M. Ho, C. T. Chan, and C. M. Soukoulis, Phys. Rev. Lett. 65, 3152 (1990).

[16] E. Yablonovitch, T. J. Gmitter, and K. M. Leung, Phys. Rev. Lett. 67, 2295 (1991).

[17] E. Yablonovitch, T. J. Gmitter, R. D. Meade, A. M. Rappe, K. D. Brommer, and J. D. Joannopoulos, Phys. Rev. Lett. 67, 3380 (1991).

[18] E. Yablonovitch, J. Opt. Soc. Am. B 10, 283 (1993).

[19] S. L. McCall, P. M. Platzman, R. Dalichaouch, D. Smith, and S. Schultz, Phys. Rev. Lett. 67, 2017 (1991).

[20] W. M. Robertson, G. Arjavalingam, R. D. Meade, K. D. Brommer, A. M. Rappe, and J. D. Joannopoulos, Phys. Rev. Lett. 68, 2023 (1992).

[21] M. Plihal and A. A. Maradudin, Phys. Rev. B 44, 8565 (1991).

[22] P. R. Villeneuve and M. Piché Phys. Rev. B 46, 4969 (1992).

[23] J. D. Joannopoulos, R. D. Meade, and J. N. Winn, Photonic Crystals Molding the Flow of Light (Princeton University Press, Princeton, 1995).

[24] A. Mekis, J. C. Chen, I. Kurland, S. Fan, P. R. Villeneuve, and J. D. Joannopoulos, Phys. Rev. Lett. 77, 3787 (1996).

[25] K. A. McIntosh, L. J. Mahoney, K. M. Molvar, O. B. McMahon, S. Verghese, M. Rothschild, and E. R. Brown, Appl. Phys. Lett. 70, 2937 (1997).

[26] S. Y. Lin, J. G. Fleming, D. L. Hetherington, B. K. Smith, R. Biswas, K. M. Ho, M. M. Sigalas, W. Zubrzycki, S. R. Kurtz, and J. Bur, Nature 394, 251 (1998).

[27] J. G. Fleming and S. Y. Lin, Opt. Lett. 24, 49 (1999).

[28] S. Noda, N. Yamamoto, H. Kobayashi, M. Okano, and K. Tomoda, Appl. Phys. Lett. 75, 905 (1999).

[29] J. D. Joannopoulos, P. R. Villeneuve, and S. Fan, Nature 386, 143 (1997).

[30] G. Parker and M. Charlton, Physics World August, 29 (2000).

[31] S. Noda, MRS Bulletin August, 681 (2001).

[32] S. Noda, M. Imada, M. Okano, S. Ogawa,M. Mochizuki, and A. Chutinan, IEEE J. Quantum Electron. 38, 726 (2002).

[33] S. Y. Lin, E. Chow, V. Hietala, P. R. Villeneuve, and J. D. Joannopoulos, Science 282, 274 (1998).

[34] T. Baba, N. Fukaya, and J. Yonekura, Electron. Lett. 35, 654 (1999).

[35] J. S. Foresi, P. R. Villeneuve, J. Ferrara, E. R. Thoen, G. Steinmeyer, S. Fan, J. D. Joannopoulos, L. C. Kimerling, H. I. Smith, and E. P. Ippen, Nature 390, 143 (1997).

[36] Y. Akahane, T. Asano, B.-S. Song, and S. Noda, Nature 425, 944 (2003).

[37] B. S. Song, S. Noda, T. Asano, and Y. Akahane, Nature Materials 4, 207 (2005).

[38] S. Noda, K. Tomoda, N. Yamamoto, and A. Chutinan, Science 289, 604 (2000).

[39] O. Painter, R. K. Lee, A. Scherer, A. Yariv, J. D. O'Brien, P. D. Dapkus, and I. Kim, Science 284, 1819 (1999).

[40] M. Imada, S. Noda, A. Chutinan, and T. Tokuda, Appl. Phys. Lett. 75, 316 (1999).

[41] R. Colombelli, K. Srinivasan, M. Troccoli, O. Painter, C. F. Gmachl, D. M. Tennant, A. M. Sergent, D. L. Sivco, A. Y. Cho, and F. Capasso, Science 302, 1374 (2003).

[42] S. Ogawa, M. Imada, S. Yoshimoto, M. Okano, and S. Noda, Science 305, 227 (2004).

[43] M. Soljačić and J. D. Joannopoulos, Nature Materials 3, 211 (2004).

[44] S. Y. Lin, J. G. Fleming, D. L. Hetherington, B. K. Smith, R. Biswas, K. M. Ho, M. M. Sigalas, W. Zubrzycki, S. R. Kurtz, and J. Bur, Nature 394, 251 (1998).

[45] J. G. Fleming and S.-Y. Lin, Opt. Lett. 24, 49 (1999).

[46] S. Y. Lin and J. G. Fleming, J. Lightwave Technol. 17, 1944 (1999).

[47] S. Noda, N. Yamamoto, H. Kobayashi, M. Okano, and K. Tomoda, Appl. Phys. Lett. 75, 905 (1999).

[48] S. Noda, N. Yamamoto, M. Imada, H. Kobayashi, and M. Okano, J. Lightwave Technol. 17, 1948 (1999).

[49] K. Aoki, H. T. Miyazaki, H. Hirayama, K. Inoshita, T. Baba, K. Sakoda, N. Shinya, and Y. Aoyagi, Nature Materials 2, 117 (2003).

[50] A. Blanco et al., Nature 405, 437 (2000).

[51] Y. A. Vlasov, X. Z. Bo, J. C. Sturm, and D. J. Norris, Nature 414, 289 (2001).

[52] M. Campbell, D. N. Sharp, M. T. Harrison, R. G. Denning, and A. J. Turberfield, Nature 404, 53 (2000).

[53] M. Maldovan and E. L. Thomas, Nature Materials 3, 593 (2004).

[54] O. Toader and S. John, Science 292, 1133 (2001).

[55] S. G. Johnson and J. D. Joannopoulos, Appl. Phys. Lett. 77, 3490 (2000).

[56] M. Qi, E. Lidorikis, P. T. Rakich, S. G. Johnson, J. D. Joannopoulos, E. P. Ippen, and H. I. Smith, Nature 429, 538 (2004).

[57] D. Roundy and J. Joannopoulos, Appl. Phys. Lett. 82, 3835 (2003).

[58] S. L. McCall, P. M. Platzman, R. Dalichaouch, D. Smith, and S. Schultz, Phys. Rev. Lett. 67, 2017 (1991).

[59] U. Gruning, V. Lehmann, S. Ottow, and K. Busch, Appl. Phys. Lett. 68, 747 (1996).

[60] H.-B. Lin, R. J. Tonucci, and A. J. Campillo, Appl. Phys. Lett. 68, 2927 (1996).

[61] T. Baba, N. Fukaya, and J. Yonekura, Electron. Lett. 35, 654 (1999).

[62] S. Noda, K. Tomoda, N. Yamamoto, and A. Chutinan, Science 289, 604 (2000).

[63] Born E. and M. Wolf. Fundamentals of Optics. Cambridge University Press, 3rd edition, 1999.

[64] P.Yeh, Optical Waves in layered Media Wiley, New York, (1988).

[65] A. Ikuo, Proc. SPIE 5069, 124 (2003).

[66] M. Kimura, K. Okahara, T. Miyamoto, J. Appl. Phys. 50, 1222 (1979).

[67] M. Sandrok, M. Wiggins, J. S. Shirk, H. Tai, A. Ranade, E. Baer, A. Hiltner, Appl. Phys. Lett 84, 3621 (2004).

[68] A. C. Edrington, A. M. Urbas, P. Derege, C. X. Chen, T. M. Swager, N. Hadjichiristidis, M. Xenidou, L. J. Fetters, J. D. Joannopoulos, Y. Fink, E. L. Thomas, Adv. Mater. 13, 421 (2001).

[69] A. L. Alvarez, J. Tito, M. B. Vaello, P. Velasquez, R. Mallavia, M. M. Sanchez-Lavez, S. Fernandez de Avila, Thin Solid Films 433, 277 (2003)

[70] M. Sandrok, M. Wiggins, J. S. Shirk, H. Tai, A. Ranade, E. Baer, and A. Hiltner, Appl. Phys. Lett. 84, 3621 (2004).

[71] S. A. Jenekhe, Ind. Eng. Chem. Fundum. 23, 425 (1984).

[72] C. J. Lawrence, Phys. Fluids. 31, 2786 (1988).

[73] D. Meyerhofer, J. Appl. Phys. 49, 3993 (1978)

[74] T. F. Krauss and T. Baba, IEEE J. Quantum Electron. 38, 724 (2002)

[75] R. M. De La Rue, Opt. Quantum Electron. 34, 1 (2002)

[76] M. Scalora, J. P. Dowling, C. M. Bowden, and M. J. Bloemer, Phys. Rev.Lett. 73, 1368 (1994)

[77] S. Radic, N. George, and G. P. Agrawal, Opt. Lett. 19, 1789 (1994).

[78] S. John and T. Quang, Phys. Rev. A 54, 4479 (1996)

[79] P. Tran, Opt. Lett. 21, 1138 (1996)

[80] A. Forchel, Nat. Mater. 2, 13 (2003)

[81] M. Soljacic, M. Ibanescu, S. G. Johnson, Y. Fink, and J. D. Joannopoulos, Phys. Rev. E 66, 055601 (2002)

[82] A. Huttunen and P. Torma, J. Appl. Phys. 91, 3988 (2002)

[83] J. Martorell, R. Vilaseca, and R. Corbalan, Appl. Phys. Lett. 70, 702, 1997.

[84] K. Sakoda and K. Ohtaka, Phys. Rev. B 54, 5742,1996

[85] T. Hattori, N. Tsurumachi, and H. Nakatsuka, J. Opt. Soc. Am. B 14, 348, 1997.

[86] N. Tsurumachi, S. Yamashita, N. Muroi, T. Fuji, T. Hattori, and H. Nakatsuka, Jpn. J. Appl. Phys. 38, 6302 1999.

[87] N. Tsurumachi, M. Abe, M. Arakawa, T. Yoda, T. Hattori, J. F. Qi, Y. Masumoto, and H. Nakatsuka, Jpn. J. Appl. Phys. 38, L1400 1999.

[88] J. Y. Ye, M. Ishikawa, Y. Yamane, N. Tsurumachi, and H. Nakatsuka, Appl. Phys. Lett. 75, 3605 1999.

[89] H. Inouye and Y. Kanemitsu, Appl. Phys. Lett. 82, 1155 2003.

[90] J. A. Rogers, Z. Bao, K. Baldwin, A. Dodabalapur, B. Crone, V. R. Raju, V. Kuck, H. Katz, K. Amundson, J. Ewing, and P. Drzaic, Proceedings of the National Academy of Sciences, 98 (9): 4835-4840, 2001.

[91] R. H. Friend, R. W. Gymer, A. B. Holmes, J. H. Burroughes, R. N. Marks,C. Taliani, D. D. C. Bradley, D. A. Dos Santos, J. L. Bredas, M. Logdlund, and W. R. Salaneck, Nature 397 (6715): 121-128, 1999.

[92] L. Eldada, R. Blomquist, L. W. Shacklette, and M. J. McFarland, Optical Engineering, 39 (3): 596-609, 2000.

[93] J. A. Rogers, M. Meier, and A. Dodabalapur, Applied Physics Letters, 73 (13): 1766-1768, 1998.

[94] L. H. Sloof, A. van Blaaderen, A. Polman, G. A. Hebbink, S. I. Klink, F. C. J. M. Van Veggel, D. N. Reinhoudt, and J. W. Hofstraat, Journal of Applied Physics, 91 (7):3955-3980, 2002.

[95] L. R. Dalton, W. H. Steier, B. H. Robinson, C. Zhang, A. Ren, S. Garner, A.Chen, T. Londergan, L. Irwin, B. Carlson, L. Field, G. Phelan, C. Kincaid, J. Amend, and A. Jen, Journal of Material Chemistry, 9 (9): 1905-1920, 1999.

[96] R.E. Slusher. Nonlinear Photonic Crystals. Springer-Verlag New York, Incorporated, 2003.

[97] V. Berger. Phys. Rev. Lett., 81:4136, 1998.

[98] N. G. R. Broderick, G.W.Ross, H.S. O erhaus, D.J. Richardson, and D.C. Hanna. Phys. Rev. Lett., 84:4345, 2000.

[99] S. Saltiel, and Yu.S. Kivshar. Opt. Lett., 25:1204, 2000.

[100] S.F. Mingaleev, and Yu.S. Kivshar. J. Opt. Soc. Am. B, 19:2241, 2002.

[101] P. A. Franken, A. E. Hill, C. W. Peters, and G. Weinreich, Phys. Rev. Lett. 7(4), 118 (1961)

[102] P. D. Maker, R. W. Terhune, M. Nisenoff, and C. M. Savage, Phys. Rev. Lett. 8(1), 21 (1962)

[103] N. Bloembergen and P. S. Pershan, Phys. Rev. 128(2), 606 (1962)

[104] S. Radic, N. George, and G. P. Agrawal, Opt. Lett. 19, 1789 (1994).

[105] G. J. Schneider, G. H. Watson, Appl. Phys. Lett. 83, 5350 (2003).

[106] M. Itoh, K. Harada, H. Matsuda, S. Ohnishi, A. Parfenov, N. Tamaoki, T. Yatagai, J. Phys. D: Appl. Phys.33, 463 (1998).